

Long-term tactile hypersensitivity after nerve crush injury in mice is characterized by the persistence of intact sensory axons

Hyoung Woo Kim^a, Sang Wook Shim^{a,b}, Anna Mae Zhao^c, Dahee Roh^a, Hye Min Han^d, Steven J. Middleton^c, Wheedong Kim^{a,b}, Sena Chung^{a,b}, Errin Johnson^e, John Prentice^f, Mike Tacon^g, Marleen J.A. Koel-Simmelink^h, Luuk Wieskeⁱ, Charlotte E. Teunissen^h, Yong Chul Bae^d, David L.H. Bennett^c, Simon Rinaldi^c, Alexander J. Davies^c, Seog Bae Oh^{a,b,*}

Abstract

Traumatic peripheral nerve injuries are at high risk of neuropathic pain for which novel effective therapies are urgently needed. Preclinical models of neuropathic pain typically involve irreversible ligation and/or nerve transection (neurotmesis). However, translation of findings to the clinic has so far been unsuccessful, raising questions on injury model validity and clinical relevance. Traumatic nerve injuries seen in the clinic commonly result in axonotmesis (ie, crush), yet the neuropathic phenotype of “painful” nerve crush injuries remains poorly understood. We report the neuropathology and sensory symptoms of a focal nerve crush injury using custom-modified hemostats resulting in either complete (“full”) or incomplete (“partial”) axonotmesis in adult mice. Assays of thermal and mechanically evoked pain-like behavior were paralleled by transmission electron microscopy, immunohistochemistry, and anatomical tracing of the peripheral nerve. In both crush models, motor function was equally affected early after injury; by contrast, partial crush of the nerve resulted in the early return of pinprick sensitivity, followed by a transient thermal and chronic tactile hypersensitivity of the affected hind paw, which was not observed after a full crush injury. The partially crushed nerve was characterized by the sparing of small-diameter myelinated axons and intraepidermal nerve fibers, fewer dorsal root ganglia expressing the injury marker activating transcription factor 3, and lower serum levels of neurofilament light chain. By day 30, axons showed signs of reduced myelin thickness. In summary, the escape of small-diameter axons from Wallerian degeneration is likely a determinant of chronic pain pathophysiology distinct from the general response to complete nerve injury.

Keywords: Axonotmesis, Chronic pain, Mechanical allodynia, Peripheral nerve injury, Neuropathic pain, Partial crush, Preclinical pain model, Wallerian degeneration

1. Introduction

Chronic pain, defined as pain lasting more than 3 months, affects more than 30% of people worldwide, placing a huge personal and economic burden on those afflicted.¹⁹ Nerve injury, either from trauma or surgery, is found in approximately 20% of chronic pain cases.²¹ In as many as 50% to 75% of these people, the pain is classified as neuropathic.⁴² Despite advances in surgical

techniques, the incidence of chronic and neuropathic pain remains high.²⁴

In 1943, Herbert Seddon produced the first clinical classification of nerve injuries,⁷⁶ which was later refined by Sidney Sunderland.⁸² A neurapraxic (transient) injury is accompanied by local myelin damage, but axons otherwise remain intact. Axonotmesis describes the severance of both axons and myelin sheaths with

Sponsorships or competing interests that may be relevant to content are disclosed at the end of this article.

A.J. Davies and S.B. Oh contributed equally to this work.

^a Department of Neurobiology and Physiology, School of Dentistry, and Dental Research Institute, Seoul National University, Seoul, Republic of Korea, ^b Department of Brain and Cognitive Sciences, College of Natural Sciences, Seoul National University, Seoul, Republic of Korea, ^c Nuffield Department of Clinical Neurosciences, University of Oxford, John Radcliffe Hospital, Oxford, United Kingdom, ^d Department of Anatomy and Neurobiology, School of Dentistry, Kyungpook National University, Daegu, Republic of Korea, ^e Sir William Dunn School of Pathology, University of Oxford, Oxford, United Kingdom, ^f Oxford Institute for Radiation Oncology, Old Road Campus Research Building, University of Oxford, Oxford, United Kingdom, ^g Department of Physics, Denys Wilkinson Building, University of Oxford, Oxford, United Kingdom, ^h Neurochemistry Laboratory, Department of Laboratory Medicine, Amsterdam Neuroscience, Neurodegeneration, Amsterdam UMC, Vrije Universiteit Amsterdam, the Netherlands, ⁱ Department of Neurology and Neurophysiology, Amsterdam UMC, Academisch Medisch Centrum, Amsterdam Neuroscience, Amsterdam, the Netherlands

*Corresponding author. Address: Department of Neurobiology and Physiology, School of Dentistry, and Dental Research Institute, Seoul National University, 101 Daehak-ro, Jongno-gu, Seoul 03080, Republic of Korea. Tel.: +82 (0)2-740-8728. E-mail address: odolbae@snu.ac.kr (S. B. Oh).

Supplemental digital content is available for this article. Direct URL citations appear in the printed text and are provided in the HTML and PDF versions of this article on the journal's Web site (www.painjournalonline.com).

Copyright © 2023 The Author(s). Published by Wolters Kluwer Health, Inc. on behalf of the International Association for the Study of Pain. This is an open access article distributed under the terms of the Creative Commons Attribution-Non Commercial-No Derivatives License 4.0 (CCBY-NC-ND), where it is permissible to download and share the work provided it is properly cited. The work cannot be changed in any way or used commercially without permission from the journal.

<http://dx.doi.org/10.1097/j.pain.0000000000002937>

intact nerve connective tissue, which remains theoretically capable of hosting axon regeneration. Neurotmesis is a complete anatomical disruption of the nerve tissue (eg, transection) in which nerve recovery does not occur without surgical intervention.⁷⁶

Nerve injuries can be associated with both negative (hypoesthesia, anaesthesia) and positive (pain, paraesthesia) sensory symptoms.⁶³ Several preclinical models have been developed to study the gain-of-function mechanisms leading to persistent pain after traumatic nerve injury.^{9,26,51,77} The most frequently used rodent models involve transection or irreversible ligation of part of the sciatic nerve (neurotmesis), designed to permanently restrict axonal regeneration. Despite great advances in our biological understanding of neuropathic pain, the field has struggled to translate findings to the clinic,⁴ resulting in calls for models that better reflect the human condition.⁶⁹

Chronic pain after trauma is more likely with nerve damage,⁶⁷ which is often incomplete⁶⁴ and consists of a mixture of neuropraxia and axonotmesis.^{61,71,83} Nerve crush injury (axonotmetic) models have long been a mainstay of loss-of-function studies of Wallerian degeneration and axonal regeneration^{1,15,16,37,66}; they are also occasionally reported to elicit pain-like behavior in rodents.^{45,85} However, discrepant observations and varying reports of either a resolving^{5,26,53} or nonresolving^{11,25} sensory phenotype have precluded the use of nerve crush in preclinical studies of neuropathic pain.

We have previously shown the development of a slow-onset mechanical hypersensitivity in a mouse model of “partial” sciatic nerve crush that does not appear after a more severe “full” crush injury.^{23,50} This suggests the presence of an inflection point in the relationship between injury severity and the outcome of positive and negative sensory symptoms that challenges previous assumptions of clinical nerve injuries.¹⁸

Here, we report a comprehensive behavioral and anatomical exploration of the partial and full sciatic nerve crush models at acute (2–7 days) and chronic (>30 days) time points in adult mice of both sexes using a simple and reproducible tool. We show that after partial crush nerve injury, there is escape of small-diameter axons from Wallerian degeneration resulting in chronic tactile hypersensitivity. Our findings provide further insights into the pathophysiology of neuropathic pain with potentially greater relevance to people with traumatic nerve injury.

2. Materials and Methods

2.1. Experimental design

All experiments were performed and reported in accordance with the ARRIVE guidelines.⁶⁸ Experiments included animals of both sexes unless otherwise indicated. Investigators performing the behavioral assessments, quantitative histological staining and morphometric analyses were blinded to the surgery group. The results were obtained from multiple independent experiments, with results obtained with the same tools confirmed in 2 different laboratories. Any mice that underwent full crush nerve injury but displayed any remaining pinprick score (>0) on the first day after surgery were considered an incomplete crush and were excluded from subsequent experiments. Otherwise, no data points were excluded from the study.

2.2. Animals

C57BL/6J mice (Jackson Laboratory, JAX, stock 000664) were purchased from DooYeol Biotech (Korea) or supplied in-house by the University of Oxford Biomedical Services unit. All experiments were conducted on 6- to 15-week-old male and female mice on

the C57BL/6J background. Mice were maintained in constant temperature (22 ± 1°C), humidity (55%), and 12-hour light/dark cycle environment with standard laboratory chow and water available ad libitum. Animal husbandry was performed in accordance with the Guideline for Animal Experiments by the Korean Academy of Medical Sciences, the National Institutes of Health Guidelines for the Care and Use of Laboratory Animals,⁶⁵ and in the United Kingdom according to the Home Office Animals (Scientific Procedures) Act 1986, revised 2012.

2.3. Crush tool development

Spacers were created out of 15- μ m-thick sheets of aluminium foil (Seong Won Cooking Foil, Cheonan, Korea). Foil thickness was confirmed using digital Vernier calipers. Foil layers were cut such that the nerve could be placed between the 2 opposing faces of the hemostat blades, bounded on both sides by one or more layers of foil to provide an aperture of varying distance between the hemostat blades (Supplemental Figure 1, available at <http://links.lww.com/PAIN/B843>). Spacers were autoclaved with hemostats for sterilization prior to surgery.

Custom modification of a series of ultrafine hemostats (Cat no. 13020-12, Fine Science Tools, Germany) was performed by sink spark erosion using bespoke copper electrodes in custom-built jig to hold the hemostats at the correct angle when closed on the first lock position. The final depth of cutout on machined hemostats were measured using an optical comparator device (IM-6700 Series, Keyence Corporation UK Ltd, Milton Keynes, United Kingdom).

2.4. Hemostat pressure measurement

Hemostats were calibrated with pressure measurement film (Prescale, Fujifilm Corporation, provided courtesy of Techni Measure, United Kingdom). Different scales of film (LW ~ 4 LW film) were placed between the blades of each hemostat in turn, which were closed for 15 seconds on the first lock position. Dye release onto film was identified as an indication the pressure across the closing face of the hemostat. The pressure range was calibrated according to the color change on each grade of film used (Supplemental Figure 1, available at <http://links.lww.com/PAIN/B843>).

2.5. Crush surgery

All surgical procedures were performed on adult mice of both sexes aged 6 to 10 weeks using aseptic technique. Mice were placed under isoflurane anaesthesia (2% induction) in 100% oxygen, weighed, and given a perisurgical injection of the analgesic agent Rimadyl (Carprofen) (5 mg/kg subcutaneously in phosphate-buffered saline [PBS]/saline). Mice were maintained on isoflurane anaesthesia at 1.5% using a face mask, with the depth of anaesthesia assessed by monitoring the breathing rate and adjusted during surgery accordingly. Body temperature was maintained with a warm pad and monitored with a rectal probe. The right thigh was shaved and iodine-treated and wiped with an alcohol Steri-Wipe. An incision was made midthigh length and the sciatic nerve exposed as it emerges from the sciatic foramen by parting the muscle with blunt forceps dissection. The sciatic nerve was carefully freed from connective tissue and gently lifted with fire-polished glass microhook. The full width of the sciatic nerve was crushed for 15 seconds using an ultra-fine hemostat placed on the first lock position (Cat no. 13020-12, Fine Science Tools). The position of the nerve crush was at midthigh level, distal from (ie, avoiding) the eminence of the posterior cutaneous femoral nerve and posterior biceps semitendinosus nerve, and proximal to the trifurcation of the sciatic nerve

into tibial, common peroneal, and sural nerve branches.^{6,52} Nerve crush injuries were performed with or without a custom foil spacer, or using engineered hemostats (Supplemental Figure 1, available at <http://links.lww.com/PAIN/B843>). Muscle fascia was then closed with one or two 7-0 silicone-coated silk or absorbable Vicryl sutures, and the skin incision was closed with 9-mm skin clips (Mikron Precision Inc., Gardena, CA). Local anesthetic (Marcain, 2 mg/kg) was administered superficially to the incision site. Animals were allowed to recover either under an infrared radiator or on a warm pad. Animals were subject to daily postsurgical monitoring and weight checks. Standard chow or mash was placed near to the cage floor to ensure easy access to food during the 7- to 10-day period of hind limb weakness after nerve injury. No unexpected adverse effects were observed as a consequence of the surgery.

2.6. Behavior

2.6.1. Evoked sensory behavior

To test tactile sensitivity and pinprick score, the mice were placed singly in transparent acrylic box or cylinder on an elevated mesh floor. Fifty percent paw withdrawal thresholds were measured following Chaplan up-down method with a series of graded von Frey filaments (0.04-2 g, Stoelting Wood Dale, IL) applied between the central footpads and lateral plantar surface of each paw. The 0.4-g filament was first stimulus to be used. A positive response was judged to be a brief lifting, flicking, and/or licking of the paw within 1 to 2 seconds after application of the filament. The response to the pinprick stimuli was scored out of 10, as previously described.²³ Briefly, the paw area (mediolateral side of hind paw) was divided into 5 separate regions to which an Austerlitz insect pin (size 000, Fine Science Tools, CA, US) was applied twice per region. A brisk withdrawal of the paw was scored as a positive pinprick response.

Thermal hypersensitivity was measured using a Hargreaves radiant heat apparatus (IITC Life Science, CA). Mice were placed in individual transparent acrylic container (8.5 × 8.5 × 17 cm) above the transparent glass floor. The basal paw withdrawal latency was adjusted to 10 to 15 seconds (initial-intensity 5, auto-intensity 25-28, Glass surface at 30°C) and a cutoff of 20 seconds was set to prevent tissue damage. Both hind paws were stimulated for 3 to 4 times with at least 20-minute intervals. The average latency was determined as final latency. The mice were habituated to the testing environment before the assessments.

2.6.2. Motor function assessment

For gross motor function analysis, the latency to fall from rotating rod was measured using a rotarod device (BS Technology Inc, Anyang, Korea). Mice were pretrained for 2 days on an automated 5-lane rotarod unit before measuring the baseline. During the testing phase, the mice were placed on the rod as it accelerated from 2 rpm to 40 rpm throughout 60 seconds. The length of time that each mouse stayed on the rotating rod was recorded automatically. The cutoff time was set at 300 seconds. The readings from 3 trials were averaged. At least 20 minutes of intervals were given between the trials. Mice that had lower baseline latency than the latency after crush injury were considered unhabituated and excluded from the data.

For sciatic functional index⁷ measurement, mice were placed on a transparent acrylic plate in a dark cage where light is cutoff from 5 sides except for the bottom. The reflection image of the bottom of the feet was acquired from the video recording of the mirror placed under the acrylic plate. A single shot from each

mouse was captured when facing forward with all 4 paws on the floor. A thresholded image of the plantar surface of both hind paws was acquired through ImageJ.

2.7. Retrograde tracer labelling

Under brief isoflurane anesthesia, 8 μ L of 3% Dil (Cat no. D282, Molecular Probes) in DMSO (Dimethylsulfoxide) was injected in the plantar surface of both hind paws at 2 days postinjury, and the DRG tissue was sampled on day 15. For a faster tracer, Fluoro-Gold (Fluorochrome, LLC) was used. Ten microliters of 2% Fluoro-Gold in saline were injected in the plantar surface of both hind paws at 30 days postinjury, and the DRG tissue was sampled on day 35. The tracer was injected in the middle of the lateral side of the hind paw within the sciatic nerve innervating area.

2.8. Immunohistochemistry

After appropriate survival times, the mice were terminally anesthetized by intraperitoneal injection of sodium pentobarbital (>400 mg/kg) and perfused transcardially with PBS followed by 4% paraformaldehyde in 0.1 M PBS. Hind paw skin was acquired from the central foot pad, corresponding to the territory innervated by the sciatic nerve using a 2-mm biopsy punch; L4 DRG were dissected from the spinal column. The fixed samples were postfixed with the same fixative at 4°C overnight. Both tissues were cryoprotected in 30% sucrose solutions and then embedded in OCT (Optimal Cutting Temperature) compound. Frozen samples were cut with a cryostat microtome (Leica, Wetzlar, Germany) into 10- μ m slices and mounted onto Superfrost glass slides. The sections were blocked and permeabilized with 5% to 10% host serum and 0.3% PBST (Triton-X 100) for 1 hour at room temperature. After being incubated with primary antibodies at 4°C overnight, the sections were then incubated with secondary antibodies and DAPI (4',6-diamidino-2-phenylindole) (1 μ g/mL; Cat no. D9542, Sigma, MO) for 1 to 2 hours at room temperature; 1% host serum in 0.03% PBST (Triton-X 100) was used as antibody diluent, and the antibodies were washed with PBS. Triton-X 100 was replaced with Tween 20 specifically for staining Dil-labeled DRG slices.

For whole mount staining of the extensor hallucis longus (EHL) muscle, the muscles were dissected out after PBS perfusion and postfixed for 15 minutes at room temperature. The fixed tissues were permeabilized with 1% PBST and blocked with 3% BSA (Bovine serum albumin) for 1 hour at room temperature. Primary antibodies were treated overnight at 4°C. Secondary antibody and α -bungarotoxin were treated for 1 hour at room temperature; 0.1% PBST was used as antibody diluent and wash. After finishing all the steps, tissues were then mounted with Vectorshield mounting media (Cat no. H-1000, Vector, CA, US) with cover glass for imaging.

2.9. Confocal fluorescence imaging and analysis

Fluorescence images were acquired on a confocal laser scanning microscope (Zeiss LSM700) using Zen Black software. For imaging activating transcription factor 3 (ATF-3) in NeuN-positive area in L4 DRG, 6 z-sections low-magnification ($\times 10$) images at 0.5 zoom were acquired and exported as maximum intensity projection. Five sections were imaged per tissue sample. Images were converted to black and white by adjusting to a set threshold for analysis. The number of ATF-3 nuclei was identified by automated quantification using particle analysis function and

normalized with the NeuN-positive area after scale calibration using ImageJ (v1.46r, NIH).

For analyses of ATF-3 expression in each sensory neuron subpopulation, 5 z-sections (2.5- μ m interval) low-magnification ($\times 20$) confocal images at 0.6 zoom were acquired and exported as maximum intensity projection. Three sections per sample were imaged for analyses. All Neuronal marker + DAPI + cells were manually counted, and then, ATF-3-expressing cells were counted among these cells. Images were acquired and analyzed by an investigator blinded to the injury group of the samples.

For analyses of retrograde tracer-labeled area in NeuN positive area, 5 z-sections (2.5- μ m interval) low-magnification ($\times 10$) confocal images at 0.6 digital zoom were acquired and exported as maximum intensity projection. After scale calibration and setting a threshold, the fluorescence positive area was measured.

For imaging intraepidermal nerve fibers (IENF), 3 tissue sections per paw, and 3 regions of interest (ROI) per section were analyzed. 10 to 12 z-sections (1- μ m interval) high-magnification ($\times 63$) confocal images at 0.5 zoom were acquired and exported as maximum intensity projections. For quantification of IENF in hind paw skin, β -tubulin III positive nerve fibers were manually counted as they crossed the basement membrane of the epidermis according to previously published guidelines.⁵⁵ The dermal-epidermal boundary in skin biopsies was identified by the high density of DAPI nuclei staining within the epidermal layer.⁵⁹ Intraepidermal nerve fibers density was defined as the number of crossing nerve fibers per length of skin on each image. Images were acquired and analyzed blind to the injury types.

For EHL motor nerve fiber innervation analysis, 26 z-sections (4- μ m interval, 100- μ m total range) low-magnification ($\times 20$) confocal images at 0.5 zoom were acquired and exported as maximum intensity projection. The whole EHL muscle were imaged in 3 to 4 images, and the number of total neuromuscular junction (NMJ) and the axon-occupied NMJ were manually counted, blind to the injury types.

2.10. Western blot

Mice were terminally anesthetized by intraperitoneal injection of sodium pentobarbital (>400 mg/kg) and perfused transcardially with PBS only. Bilateral sciatic nerves were rapidly dissected, snap frozen in liquid nitrogen, and stored at -80°C . Fresh, frozen, sciatic nerve tissues were homogenized in RIPA buffer (Cat no. 20-188, Millipore, MA) containing protease inhibitor cocktail (Cat no. P8340, Sigma) and phosphatase inhibitor cocktail (Cat no. P3200, Gendepot, TX). Protein samples were purified by centrifugation (13,000 rpm, 10 minutes). Equal amount of protein samples (30-40 μ g) was separated by sodium dodecyl sulfate polyacrylamide gel electrophoresis (5% stacking gel, 10% resolving gel) followed by transfer to a PVDF (polyvinylidene fluoride) membrane. Membranes were blocked with 5% skimmed milk at room temperature for 1 hour and subsequently incubated with primary antibodies diluted in the blocking solution overnight at 4°C . HRP (horseradish peroxidase)-conjugated secondary antibodies were diluted in the blocking solution and incubated for 1 hour at room temperature. Tris-buffered saline containing 0.1% Tween 20 (TBS-T) was used as blocking/antibody diluent and wash. Blots were developed by application of western ECL substrate (Catno. 1705061, BioRad, CA). The images of sequential exposure times were acquired digitally (ChemiDoc, BioRad), and the density of the protein bands were analyzed with Image Lab Software (version 4.1).

Antibodies used for immunostaining and western blot are listed in the Supplemental Table 1, available at <http://links.lww.com/PAIN/B843>.

2.11. Resin embedding of sciatic nerves

Mice were terminally anesthetized by intraperitoneal injection of sodium pentobarbital (>400 mg/kg) and perfused transcardially with 0.85% NaCl solution, followed by paraformaldehyde/glutaraldehyde fixative (1% paraformaldehyde, 2.5% glutaraldehyde, 0.1% picric acid in 0.1 M PB, pH 7.4) for 15 minutes. The distal sciatic nerve tissue from the crush site was isolated and postfixed for 2 hours in the same fixative at 4°C temperature. Tissues were treated with 1.0% to 1.5% OsO₄ in 0.1 M PB for 1 to 2 hours at room temperature, and dehydrated through a graded series of ethanol washes (30%-100%, 30 minutes each). Tissues were then transferred through propylene oxide to epoxy resin (Durcupan ACM, Fluka, Buchs, Switzerland, or Taab, T028, medium resin) for embedding in resin coffins and cured for 48 hours at 60°C .

2.12. Semithin sectioning and analysis

For day 2 nerve samples, semithin sections (500 nm) were mounted on Superfrost slides and stained with toluidine blue (0.5%) for 90 seconds followed by rinsing with tap water. Air-dried slides were then mounted with nonaqueous mountant (DPX). Sections were imaged on a Leica DM500 microscope fitted with a X100 oil-immersion lens (1.25 NA, PLAN, Leica) and CCD (Basler, Ahrensburg, Germany). Whole cross-sections of sciatic nerve were digitised with online stitching using Manual Whole Slide Imaging (WSI) software (2019B, Microvisioneer). Myelinated axons were quantified in five 50 μ m \times 50 μ m regions of interest (ROI) per nerve by an experimenter blinded to experimental group. Myelinated axons were measured using a publicly available plugin (<http://gratio.efil.de/>) for Fiji/ImageJ,³⁹ and axon diameter, myelin thickness, and g-ratio were calculated from measured area based on assumption of circularity (diameter = $2 \times \sqrt{[\text{area}/\pi]}$).

2.13. Ultrathin sectioning, transmission electron microscopy, and analysis

For day 2 (n = 3 full crush, n = 4 partial crush), and day-7 nerve samples (n = 6 full crush, n = 6 partial crush), ultrathin sections (90 nm) were transferred to formvar-coated 50 copper slot grids and poststained for 5 minutes with uranyl acetate and lead citrate. Grids were imaged at 120 kV in either a FEI Tecnai 12 TEM or JEOL 1400 TEM using a Gatan OneView camera at $\times 900$ magnification for myelinated fibre analysis (12-13 images per nerve) and $\times 2900$ to $\times 3000$ magnification for unmyelinated fibre analysis (10 images per nerve). For day 30 samples, samples were cut at 70 nm and collected on formvar-coated single slot nickel grids and stained with uranyl acetate and lead citrate. Electron micrographs were taken at random from the sciatic nerve cross-section area (8 electron micrographs per nerve: $24.40 \times 20.57 \mu\text{m}/\text{image}$). Axon diameter and g-ratio were measured as above. For unmyelinated fibre analysis, individual Remak bundles were identified by axons surrounded by the basal lamina of a dark Schwann cell cytoplasm. All axons were analyzed or counted by an investigator blind to the experimental group.

2.14. Simoa

Peripheral blood was collected from the tail vein by making a small incision in the lateral tail vein after swabbing with a disinfectant wipe. Two to three drops of blood (approx. 30 μ L) were collected in a sterile Eppendorf tube. The tubes were maintained at room temperature for 30 to 60 minutes to allow coagulation and then

centrifuged at 2000g for 25 minutes. The upper serum layer was collected and kept at -80°C until analysis. Before analysis, samples were thawed at room temperature and centrifuged at 10,000g. Subsequently, serum NfL concentrations were determined in accordance with manufacturer guidelines using Simoa NF-light advantage kit (Quanterix, MA).

2.15. Literature keyword analysis

Research papers were grouped into transection, ligation, constriction, compression, or crush nerve injuries in nonhuman animals using a keyword search on the National Library of Medicine PubMed database hosted by the National Institutes of Health, United States (last searched October 2022). “Pain[Title/Abstract],” “Nerve injury,” “Model,” and NOT “Spinal cord injury” were used for sorting out pain research from nerve injury models, and “Regeneration[Title/Abstract],” NOT “Pain[Title/Abstract],” “Nerve injury,” “Model,” NOT “Spinal cord injury,” NOT “brain,” and NOT “in vitro” were used for regeneration research. “Other animal” filter was applied. For pain research articles, the keyword “Crush” for crush injury, “Compression” for compression, “Transection” and NOT “Ligation” for transection injury, and “Ligation” NOT “Constriction” for ligation injury were used. For regeneration articles, the keyword “Crush,” “Transection,” “Ligation” NOT “Transection,” “Compression” NOT “Crush,” and “Constriction” were used. Review articles or irrelevant fields of study were manually excluded.

2.16. Statistics

A power calculation was performed using In Vivo Stat software⁹ to determine the sample size required in behavioral assays to achieve a minimum significance level of 5% and power of 80%. For example, to detect a difference in thermal withdrawal threshold of 5 seconds from baseline with an average SD of 3 seconds would require 7 animals. For detecting an average difference in mechanical sensitivity thresholds (0.17 g) and average SD of 0.1 g, a sample size of 8 animals would achieve a power of 90%. Preliminary data assessing ATF3 expression after nerve crush injury was used to determine a sample size of 6 per group (3–4 tissue sections averaged per animal) would be required to detect meaningful differences by quantitative immunohistochemistry. Data from multiple samples were averaged per animal before analysis. Comparisons between 2 groups (eg, full vs partial crush) were made with Student unpaired *t* test where normally distributed (2-tailed unless otherwise stated). Comparisons between 3 groups, where appropriate, were made with 1-way ANOVA (Analysis of Variance) with Tukey posttest. Two-way ANOVA with post hoc tests, to correct for multiple comparisons, was used to compare the effects of surgery on behavioral assays over time. $P < 0.05$ was considered significant. Analyses were performed using GraphPad Prism v8 or 9 (GraphPad Software). Two sample Kolmogorov–Smirnov test (“ks.test()” function) for single-axon analyses was performed with R package dgof, available on CRAN (<https://github.com/cran/dgof>).³ Data points represent average values from individual mice unless otherwise stated, with mean and standard error of the mean (SEM) superimposed for each group.

2.17. Study approval

All experimental procedures were approved by the Institutional Animal Care and Use Committee at Seoul National University (protocol code: SNU-200506-1-3). Procedures performed at the University of Oxford were performed in accordance with the UK

Animal (Scientific Procedures) Act 1986 under a Home Office project licence (P1DBEBAB9).

3. Results

3.1. Representation of crush injury in the neuropathic pain literature

We first identified the prevalence of preclinical nerve injury models used in publications related to either pain or nerve regeneration research using a keyword search on the National Library of Medicine PubMed database. Constriction injury was the most frequently used in pain research articles, followed by nerve ligation (**Fig. 1A**), whereas crush injury was the most commonly used for studies of nerve regeneration (**Fig. 1B**). Nerve transection was largely used for investigating axonal regeneration after surgical nerve repair, but it also appears in pain models in place of, or in addition to, nerve ligation. These results demonstrate a significant disparity in the types of peripheral nerve injury models used within the pain and nerve regeneration fields.

3.2. Development of full and partial crush injury models

To develop the crush injury as a reproducible model of neuropathic pain, we first optimized the partial crush tool. An initial sciatic nerve partial crush prototype tool was produced by separating the blades of an ultrafine hemostat with an aluminum foil spacer (Supplemental Figure 1A, available at <http://links.lww.com/PAIN/B843>). A cohort of mice underwent a single, unilateral, sciatic nerve crush for 15 seconds on the first lock position using the same hemostat fitted with multiple layers of 15- μm -thick aluminium foil to produce different degrees of incomplete nerve crush injury. Crush using a single layer of the foil (15 μm) as spacer resulted in the complete loss of sensitivity to pinprick in the affected paw for up to 3 days after injury, a behavioral response that was indistinguishable from full crush (0- μm spacer). We observed that 30 μm was the minimum spacer that resulted in an early sensory pinprick response distinguishable from a “full” crush injury (Supplemental Figure 1B, available at <http://links.lww.com/PAIN/B843>). Despite a variation in the tip width (range 0.6–1.0 mm) of commercially available hemostats (Supplemental Figure 1C, available at <http://links.lww.com/PAIN/B843>), spacer thickness was the key determinant of sensory loss after crush injury (Supplemental Figure 1D, available at <http://links.lww.com/PAIN/B843>). Using precision tooling, we engineered a series of hemostats with low tolerance in spacer gap ($27.67 \pm 3.67 \mu\text{m}$, $n = 6$) (Supplemental Figure 1E, available at <http://links.lww.com/PAIN/B843>). The early onset pinprick response (Supplemental Figure 1F, available at <http://links.lww.com/PAIN/B843>) and delayed-onset tactile hypersensitivity (Supplemental Figure 1G, available at <http://links.lww.com/PAIN/B843>) after partial crush were indistinguishable when induced by either the foil-based prototype or precision-tooled hemostat. We observed that a number of the unengineered hemostats (3/6) required tooling to create fully opposing blades (0- μm spacing) and thus guarantee a full crush. To better understand the physical forces applied to the sciatic nerve, we calibrated the hemostats with different scales of pressure measurement film (Supplemental Figure 1H, available at <http://links.lww.com/PAIN/B843>). The results show that the hemostat blades, when fully opposed and placed on the first lock position, apply a pressure of between 0.5 and 2.5 MPa, which equates to approximately 5 to 25 kgf/cm^2 . No pressure was recorded at the partial crush site due to the space in the hemostat blades (Supplemental Figure 1H, available at <http://links.lww.com/PAIN/B843>).

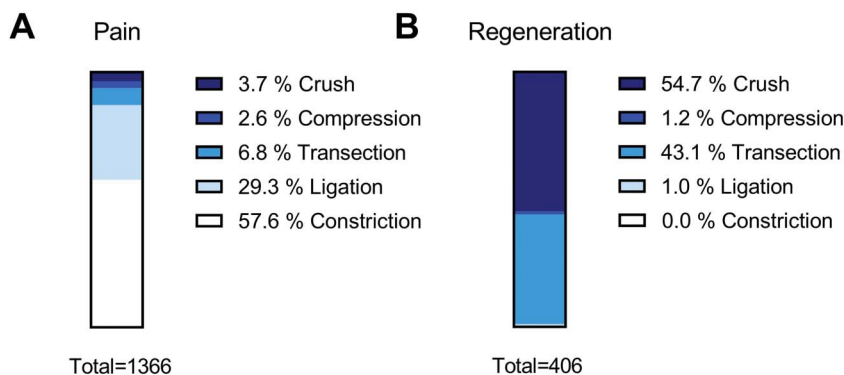


Figure 1. Prevalence of peripheral nerve injury models used in pain and regeneration research. (A) The number of articles using each nerve injury models for pain research since 2000/08/01 (B) The number of articles using each nerve injury models for regeneration research since 2000/08/01. Chi-squared contingency, $P < 0.0001$. Data are presented as percentage of total publications in each field.

3.3. Differential sensory response between crush models

We first examined the temporal pattern of mechanical and thermal sensitivity in the 2 crush models in both male and female mice (**Fig. 2A**). Consistent with previous observations,²³ the time course of the recovery of the sensory response to pinprick varied between the crush injuries (**Figs. 2B and C**). Full-crush injury resulted in a transient tactile *hyposensitivity* of the plantar surface of the ipsilateral hind paw on the first week after the surgery that recovered to baseline threshold after approximately 2 weeks (**Figs. 2D and E**). Partial crush injury resulted in reduced mechanical thresholds from 2 weeks that lasted over 60 days postinjury (**Figs. 2D and E**); the frequency of response to a single von Frey filament also remained elevated at day 28 compared with full crush (Supplemental Figure 2A, available at <http://links.lww.com/PAIN/B843>). Mice showed relative insensitivity to thermal stimuli following full crush injury for a period of approximately 3 days and recovered to baseline within a week, reminiscent of nerve crush injury in the rat, which does not develop signs of a painful syndrome.⁷⁹ By contrast, in partial crush nerve-injured mice, thermal thresholds transitioned to thermal *hypersensitivity* from day 6 (**Figs. 2F and G**), coinciding with the early appearance of pinprick response in this model (**Figs. 2B and C**). Unlike tactile sensitivity, the thermal hypersensitivity to partial crush nerve injury resolved within 28 days (**Figs. 2F and G**). Overall, sensory behaviors to evoked stimuli observed after respective crush nerve injuries were comparable between male (**Figs. 2B, D and F**) and female (**Figs. 2C, E and G**) mice; data from both sexes were therefore grouped in subsequent experiments. Interestingly, the frequency of response to repeated von Frey stimulation of the contralateral hind paw was also elevated 28 days after partial crush nerve injury compared with full crush injury (Supplemental Figure 2B, available at <http://links.lww.com/PAIN/B843>), although the sensitivity thresholds of the contralateral paw did not change significantly during the study in either sex for tactile (Supplemental Figure 3A and C, available at <http://links.lww.com/PAIN/B843>) and thermal stimuli (Supplemental Figure 3B and D, available at <http://links.lww.com/PAIN/B843>).

3.4. Differential denervation of sensory axons between crush models

We examined intraepidermal nerve fiber (IENF) density of the hind paw skin following crush nerve injury (**Fig. 3A**). As expected from the known time course of Wallerian degeneration,²⁰ there was a

significant loss of IENFs in the plantar surface of the hind paw innervated by the sciatic nerve on day 2 with no fibres detectable by day 7 after full crush (**Fig. 3B**). In comparison, there were significantly more IENFs at all time points after partial crush (**Fig. 3B**). By day 30 postinjury, there was some signs of reinnervation of IENF in the full crush injury group, although there were still fewer fibers compared with the partial crush model (**Fig. 3B**). We next examined the integrity of sensory axons from the hind paw to the dorsal root ganglia (DRG) by the injection of fluorescent tracers into the hind paw skin 2 days or 30 days after the crush injury (**Fig. 3C**). Following Dil injection at day 2, few Dil-positive sensory neurons were observed in L4 DRG by the time of sampling (day 15) after full crush, suggesting a complete severance of afferent fibres (ie, axonotmesis) by the time of injection (**Fig. 3D**). By contrast, retrograde Dil labelling in L4 DRG at the same time point was significantly greater after partial crush (**Fig. 3E**), indicating the continuity of at least a subset of sensory axons. The number of fluorogold (FG)-positive neurons in L4 DRG following injection at day 30 was also greater in the partial crush model (**Figs. 3F and G**) implying that despite regeneration, peripheral innervation following partial crush remains greater than after full crush.

3.5. Motor axons are equally affected between crush models

Next, we investigated sciatic nerve motor function following the 2 crush nerve injuries. Both sexes showed a temporal reduction in the sciatic functional index (SFI) over time—as measured by the change in toe spread pattern⁷—consistent with an initial loss of function that was indistinguishable between full and partial crush injuries (**Fig. 4A**). Gross motor function was evaluated by measuring the latency to fall from accelerating rotor-rod and was not significantly different between the 2 models (**Fig. 4B**).

Motor nerve innervation of the extensor hallucis longus (EHL) muscle, supplied by the sciatic nerve, was measured by the percentage colocalization of synapsin-positive motor fiber endings with the NMJ marker, alpha bungarotoxin (α -BTx), on days 2, 7, and 30 (**Fig. 4C**). Neuromuscular junction innervation was completely absent in both full and partial crush injury models on day 2 and fully recovered by day 30; there were no significant differences between the 2 groups (**Fig. 4D**). These results suggest that peripheral motor axons are fully denervated in both crush models, in line with the similar loss of motor function in the 2 groups. Surprisingly, when injury models were grouped together, female mice showed a slower recovery to full motor function in

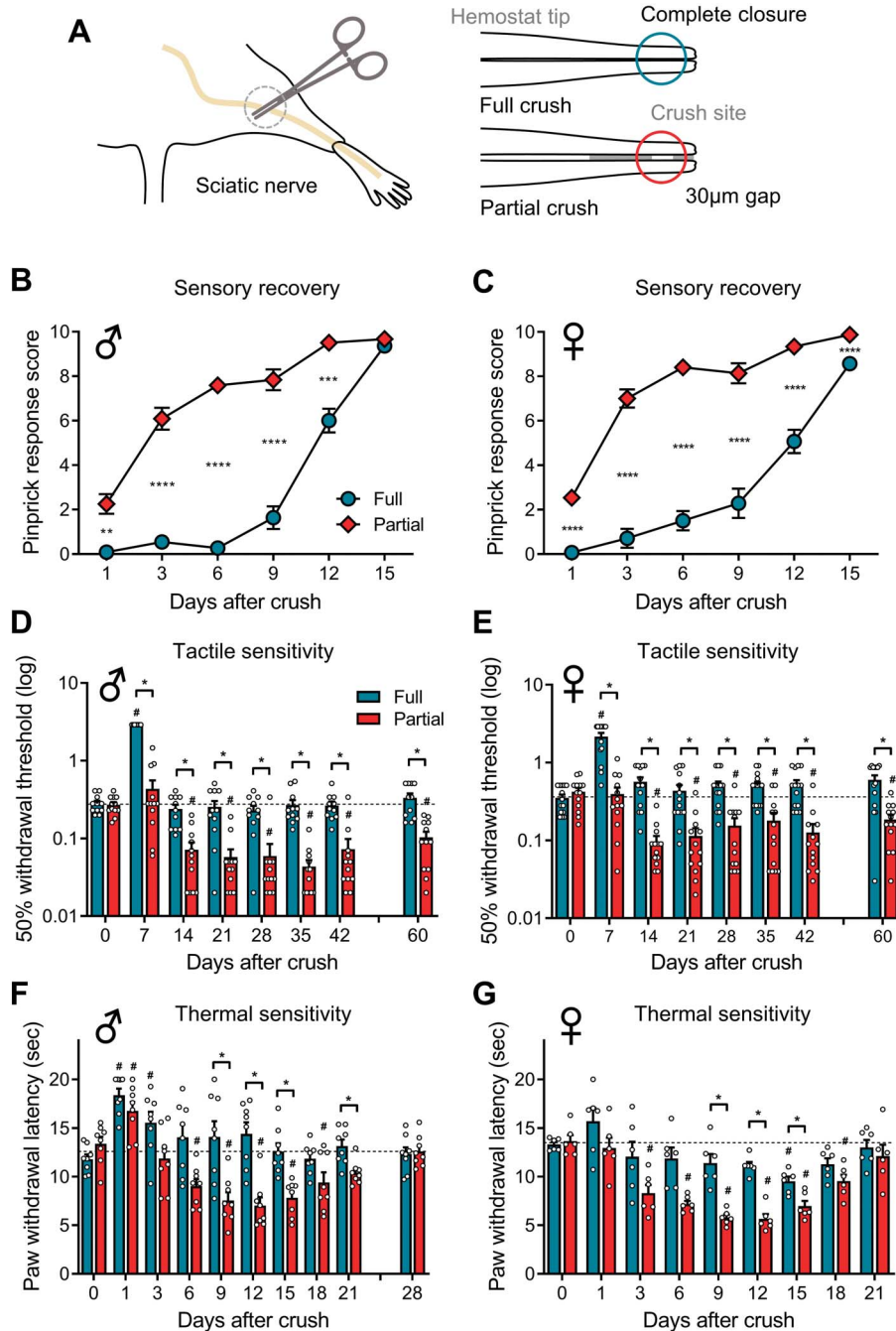


Figure 2. Hypersensitivity following incomplete loss of sensory function after nerve crush injury. (A) Schematic representation of the crush site and tool to produce full and partial crush injury. (B) Ipsilateral pinprick response score measured every 3 days after full and partial crush injury in male mice. Effect of surgery $F(1, 21) = 220.5, P < 0.0001$; full $n = 11$; partial $n = 12$ mice. (C) Pinprick score in female mice. Effect of surgery $F(1, 27) = 157, P < 0.0001$. (D) 50% withdrawal threshold of ipsilateral paw measured weekly after full and partial crush injury in male mice. Effect of surgery $F(1, 21) = 406.9, P < 0.0001$; full $n = 11$; partial $n = 12$ mice. (E) 50% withdrawal threshold of ipsilateral paw in female mice. Effect of surgery $F(1, 25) = 83.93, P < 0.0001$; full $n = 14$; partial $n = 13$ mice. (F) Ipsilateral paw withdrawal latency measured every 3 days after full and partial crush injury in male mice. Cutoff time was set at 20 seconds. Effect of surgery $F(1, 14) = 41.17; P < 0.0001$; full and partial $n = 8$ mice each. (G) Paw withdrawal latency in female mice. Effect of surgery $F(1, 10) = 55.08; P < 0.0001$; full and partial $n = 6$ mice each. (B–G) Two-way Repeated measures (RM) ANOVA with Sidak multiple comparisons; * $P < 0.5$ and Dunnett multiple comparison vs day 0; # $P < 0.5$. A dotted line is an average of the baseline threshold or latency. Data are presented as means \pm SEM.

comparison to male mice (Supplemental Figure 4A, available at <http://links.lww.com/PAIN/B843>), although there was no observable sex difference in NMJ innervation at either of the time points tested (Supplemental Figure 4B, available at <http://links.lww.com/PAIN/B843>). Together, these results suggest that the immediate loss of motor function is equivalent between full and partial crush models but that motor recovery may be sex dependent.

3.6. Differential axonal degeneration between crush models

Next, we assessed axon fiber continuity within semithin and ultrathin cross-sections of the sciatic nerve distal to the site of injury (> 10 mm) in both models. In a pilot experiment, semithin sections sampled 2 days after crush injury were stained with toluidine blue (Supplemental Figure 5A, available at <http://links.lww.com/PAIN/B843>). Despite clear signs of injury, myelin profiles were still relatively intact in both injury

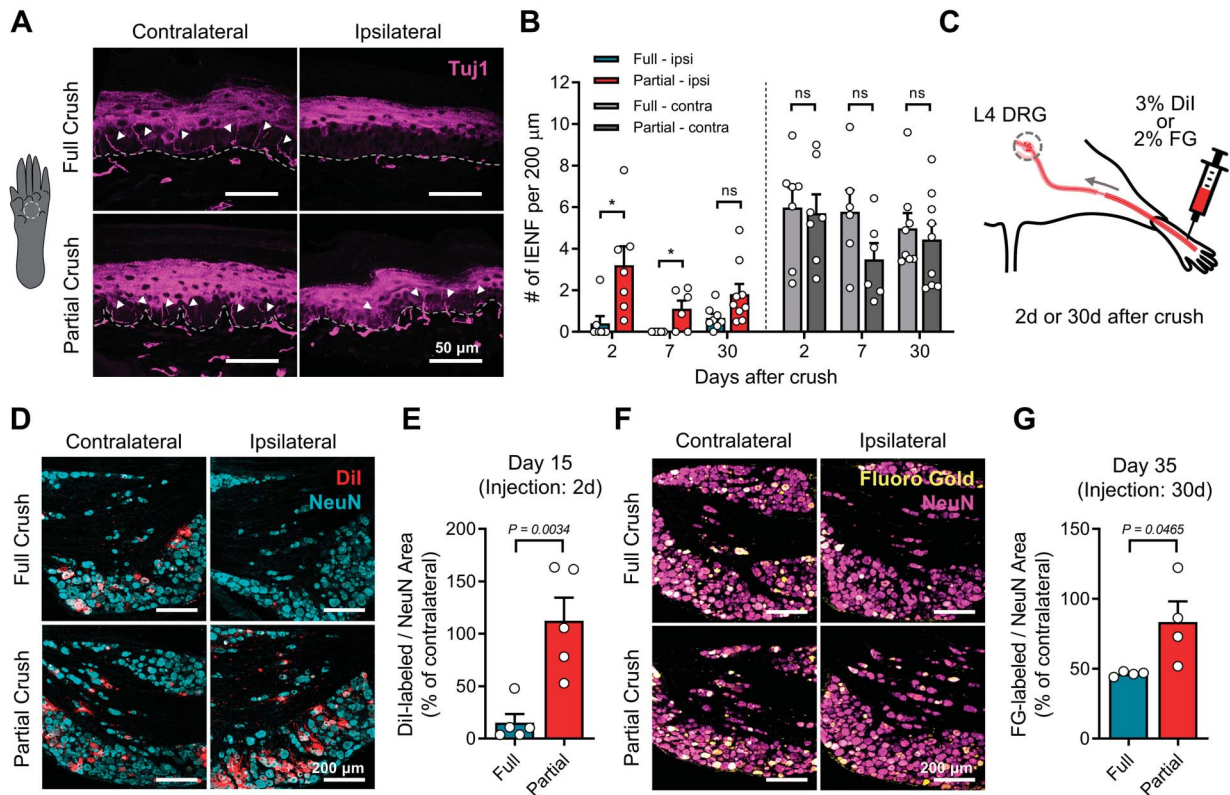


Figure 3. Peripheral sensory innervation remains intact after partial crush injury. (A) Representative images of skin IENF 7 days after crush injury. Location of hind paw plantar skin biopsy shown on left. Dashed lines indicate location of the epidermal basement membrane. (B) Number of IENF per 200- μm skin length on day 2 ($*P = 0.0144$), day 7 ($*P = 0.0181$), and day 30 ($P = 0.0531$). Unpaired *t* test. Two-tailed. $n = 6$ to 9 mice per group; 5 skin sections per mouse were analyzed. (C) Schematic image of retrograde tracer labeling strategy. (D) Representative images of L4 DRG 13 days after Dil labeling (Red) stained with NeuN (Cyan). (E) Percentage of Dil-labeled area per NeuN-positive area on day 15. Data are normalized with the percentage of the contralateral labeling. $n = 5$ each group. (F) Representative images of L4 DRG 5 days after FG-labeling (yellow) stained with NeuN (magenta). (G) Percentage of FG-labeled area per NeuN-positive area on day 35. Data are normalized with the percentage of labeling in the contralateral DRG. $n = 4$ mice per group. Three tissue sections were analyzed per mouse. (B, E, G) Unpaired *t* test, two-tailed. Data are presented as mean \pm SEM. DRG, dorsal root ganglia; FG, fluorogold; IENF, intraepidermal nerve fibers.

models. We observed a trend for a greater change in the g-ratio profile and slope after full crush compared with the uninjured nerve, although this did not reach significance in comparison to partial crush (Supplemental Figure 5B and C, available at <http://links.lww.com/PAIN/B843>). There was no change to the average g-ratio (Supplemental Figure 5D, available at <http://links.lww.com/PAIN/B843>), although the axon g-ratio distribution was more spread after the full crush injury at this time point (Supplemental Figure 5E, available at <http://links.lww.com/PAIN/B843>). Myelinated axon density was reduced 2 days after injury compared with control but was not different between the crush groups (Supplemental Figure 5F, available at <http://links.lww.com/PAIN/B843>), and there was no significant change in the average myelinated axon diameter or overall distribution (Supplemental Figure 5G and H, available at <http://links.lww.com/PAIN/B843>). These data suggested a potential delay to the onset of Wallerian degenerative changes in the partial crush compared with the full crush model, although sample sizes are likely underpowered to detect any significant differences.

High-resolution TEM (transmission electron microscopy) images of nerves 2 days postinjury revealed that the mean unmyelinated axon density was lower compared with uninjured contralateral nerves but was not significantly different between full and partial crushed nerves ($P = 0.7514$) (Supplemental Figure 6A and B, available at <http://links.lww.com/PAIN/B843>). The mean unmyelinated axon diameter was not significantly different between the groups (Supplemental Figure 6C, available at <http://links.lww.com/PAIN/B843>). However, the

frequency distributions of unmyelinated axon diameters were significantly different between full and partial crushed nerve, with a higher median axon diameter in partial crushed nerves (0.59 μm) compared with full crush (0.53 μm) and uninjured contralateral nerves (0.56 μm) (Supplemental Figure 6D and E, available at <http://links.lww.com/PAIN/B843>). There was no significant difference in axons per Remak bundle between the groups, although it tended to decrease for the injury groups (Supplemental Figure 6F, available at <http://links.lww.com/PAIN/B843>). There were significantly less Remak bundles per unit area in full crush compared with contralateral nerves ($P = 0.0309$) but no difference between other groups (Supplemental Figure 6G, available at <http://links.lww.com/PAIN/B843>). Overall, these data suggest a significant loss of unmyelinated axons after both crush injuries, with a trend for larger diameter axons in more Remak bundles after partial crush compared with full crush injury.

By 7 days after crush injury, we observed significant disruption of myelinated axons in both models (Fig. 5A). Pairwise comparison revealed a greater number of myelinated axons surviving intact after the partial crush injury than the full crush injury (Fig. 5B). There was an almost complete loss of myelinated axons larger than 4 μm in both crush models (Fig. 5C), and although the average diameter of the surviving axons was not different between the groups (Fig. 5D), the size distribution of surviving axons was shifted to the left in the partial crush model (median 2.05 μm) compared with full crush (2.47 μm) and

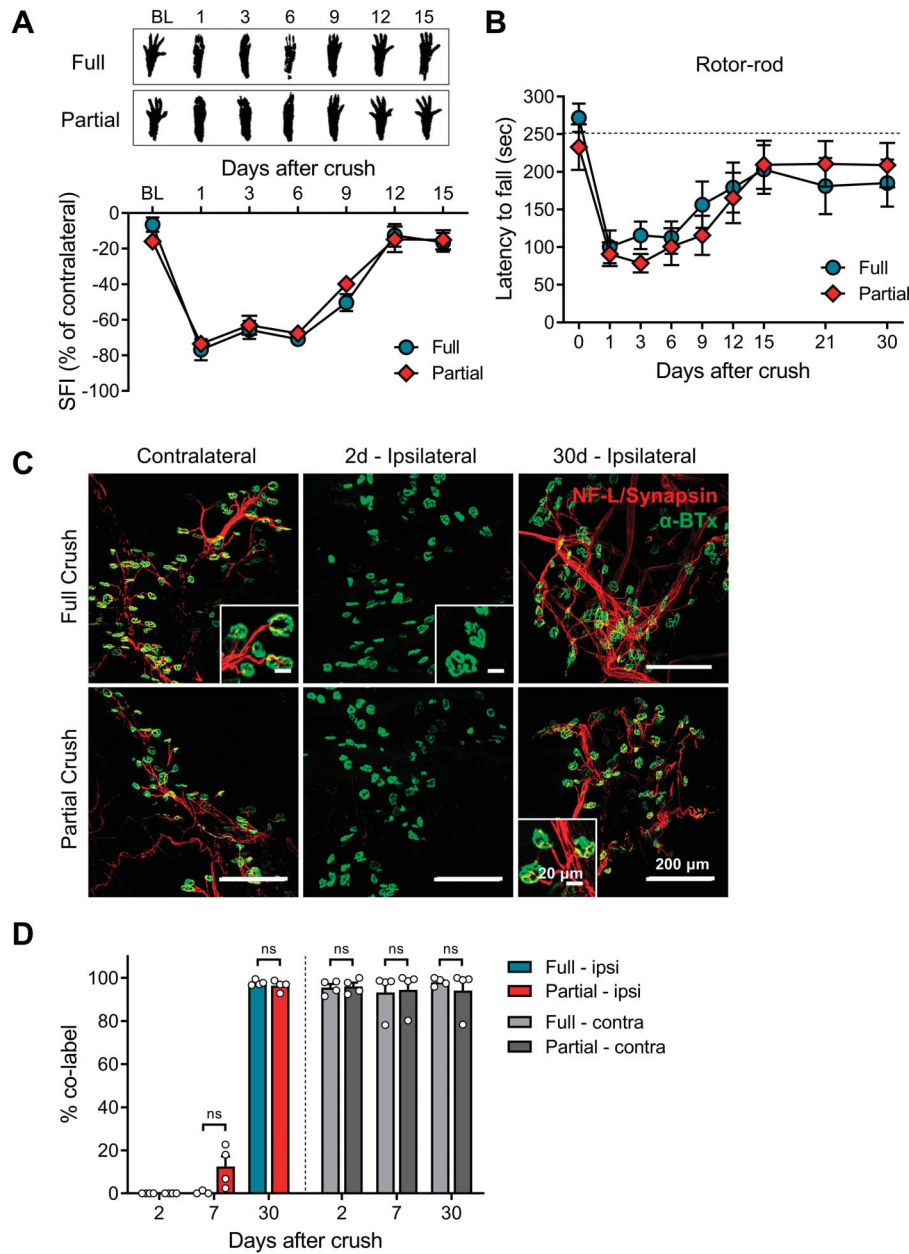


Figure 4. Complete loss of motor function and innervation after both crush injuries. (A) Representative images of ipsilateral footprints acquired every 3 days after injury and the Sciatic Functional Index (SFI) in both sexes. Effect of surgery $F(1, 29) = 0.2028, P = 0.6559$; full: $n = 15$; partial: $n = 16$. (B) Rotor-rod test after the crush injury in both sexes after full and partial crush. Time spent to fall from the rotating rod has been measured. Cutoff time was set at 300 seconds. A dotted line is an average of the baseline latency. Effect of surgery $F(1, 17) = 1.232, P = 0.7299$; full: $n = 9$; partial: $n = 10$ mice. Two-way RM ANOVA. (C) Representative images of NMJ in extensor hallucis longus (EHL) muscle 2 and 30 days after crush injury. Motor nerve fibers are stained with neurofilament light and synapsin (red), and NMJ were stained with α -bungarotoxin (green). (D) Percentage of motor nerve fibers colabeled with NMJ in EHL muscle on days 2, 7, and 30. $n = 3$ to 4 mice per group per time point. Unpaired t test. Two-tailed. ns; $P > 0.05$. Data are presented as mean \pm SEM. NMJ, neuromuscular junction.

uninjured contralateral (2.56 μ m) (Fig. 5C). Conversely, the average g-ratio of the surviving axons was significantly greater in the partial crush than the full crush model (Fig. 5E) and showed a distribution skewed to the right compared with uninjured contralateral control nerve, as well as full crushed nerves (where the g-ratio distribution collapsed) (Fig. 5F), suggesting the surviving axons in the partial crushed nerve were small diameter with thinner myelination.

Unmyelinated axons were also analysed in higher magnification TEM images at day 7 (Supplemental Figure 7A, available at <http://links.lww.com/PAIN/B843>). Although the density of unmyelinated axons was not different overall (Supplemental

Figure 7B, available at <http://links.lww.com/PAIN/B843>), there were fewer axons per Remak than uninjured controls, but this did not differ significantly between the injury models (Supplemental Figure 7C, available at <http://links.lww.com/PAIN/B843>). Average unmyelinated axon diameter showed an increasing trend after injury in both models (Supplemental Figure 7D, available at <http://links.lww.com/PAIN/B843>), likely because of the presence of regenerating large fibres (see arrow heads in Supplemental Figure 7A, available at <http://links.lww.com/PAIN/B843>). Overall, the median diameter of unmyelinated axons was lower after full crush compared with both partial crush and uninjured controls (Supplemental

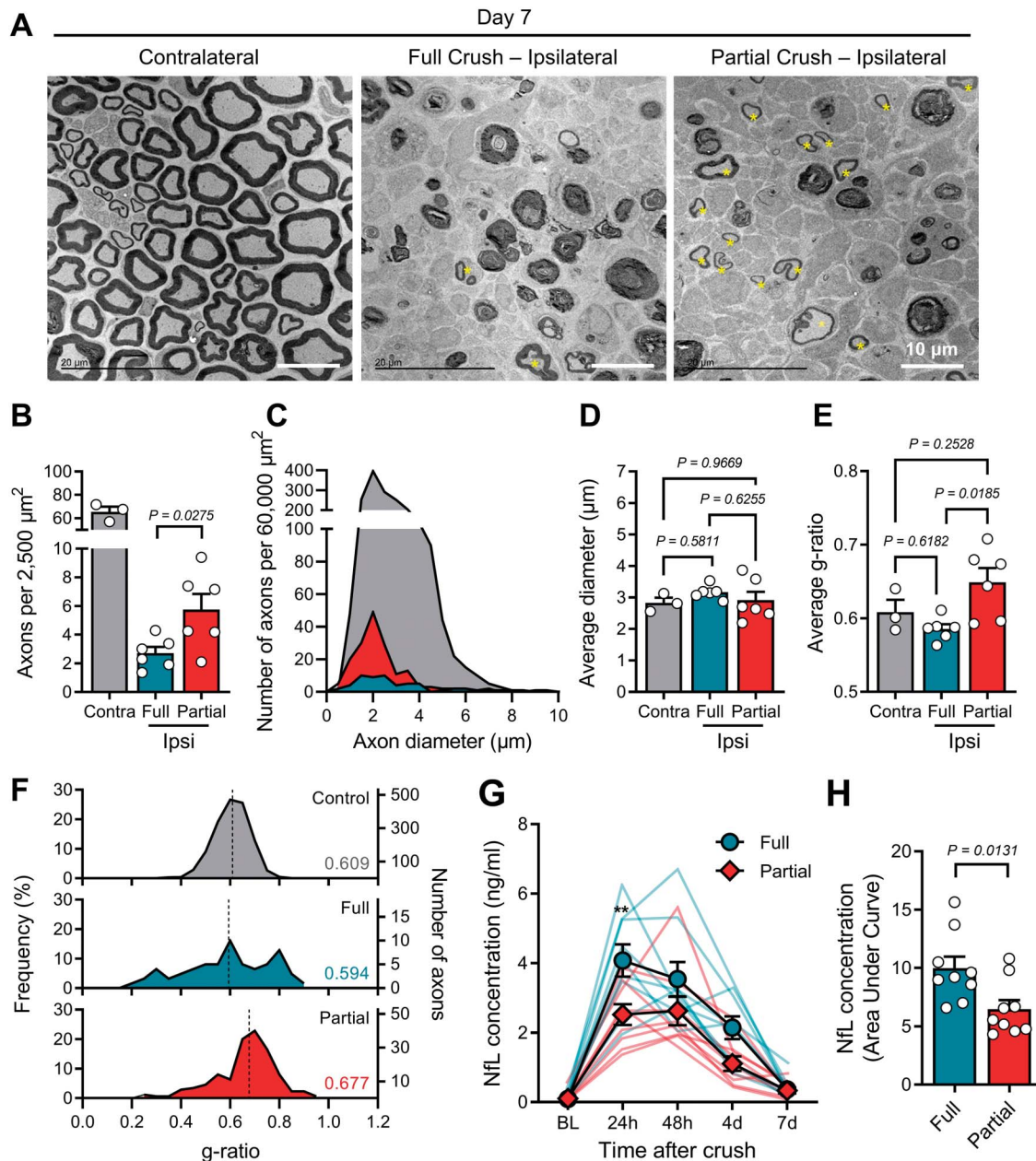


Figure 5. Small-diameter myelinated axon profiles survive more than 7 days after partial but not full crush injury. (A) Low-magnification TEM images of sciatic nerve of >10 mm distal from the crush site. The asterisk indicates surviving myelinated fibers. (B) The average number of myelinated axons per unit area. Unpaired t test. Two-tailed. (C) Absolute frequency distribution of axon diameter obtained from same area ($60,000 \mu\text{m}^2$) per group. (D) The average diameter of myelinated axons. (E) The Average g-ratio of the axons. (F) Frequency histogram of g-ratio. The dashed line and the value inside the graph indicate the median g-ratio. Two sample Kolmogorov–Smirnov test. Two-sided. Full vs Partial: $D = 0.33493$, $P = 6.923e-05$; Contra vs Full: $D = 0.27846$, $P = 0.0001848$; Contra vs Partial: $D = 0.38117$, $P < 2.2e-16$. (G) Measurement of neurofilament light chain (NfL) in serum following nerve crush injury. Effect of surgery $F(1, 80) = 13.94$, $P = 0.0004$. Two-way ANOVA with Sidak multiple comparisons; ns, $P > 0.05$, $**P < 0.01$. $n = 9$ each group. BL; Baseline. (H) Area under curve of repeated NfL measurement. Unpaired t test. Two-tailed. (B, D, E) One-way ANOVA with Tukey multiple comparisons. P values are shown above each graph. Values are average of all axons measured in 10 images per sample. Contra $n = 3$, Full $n = 6$, Partial $n = 6$ mice. Data are presented as means \pm SEM. (C and F) Total axons measured in 24 individual $50 \times 50 \mu\text{m}$ images per group (Contra $n = 1768$, Full $n = 62$, Partial $n = 175$ axons) from $n = 3$ Contra, $n = 6$ Full crush and $n = 6$ Partial crush nerve samples.

Figure 7E, available at <http://links.lww.com/PAIN/B843>, possibly suggesting greater axon outgrowth or sprouting.

Neurofilament light chain (NfL) is a key component of the axon cytoskeleton, which has been widely used as a clinical biomarker of axonal damage.⁷² Serial serum NfL concentration was measured before surgery and at 1, 2, 4, and 7 days after crush injury using the Simoa assay. Overall, the serum NfL level was higher in the full crush than the partial crush injury (Figs. 5G and H), with levels in both models returning to baseline within 7 days

(Fig. 5G). These data suggest an overall reduction in axonal degeneration but not prolongation of Wallerian degeneration after the partial crush nerve injury.

3.7. Differential expression of injury-responsive markers in sensory neurons between crush models

Activating transcription factor 3 is upregulated in a variety of stress conditions, including axotomy in sensory and motor

neurons.⁸⁴ We first assessed the overall number of ATF3-positive nuclei in L4 DRG tissue at 3 time points after the 2 crush injuries. Between days 2 and 7, we observed a progressive increase in the number of ATF3-positive nuclei in the ipsilateral L4 DRG soma area of both crush injury groups. However, the partial crush group displayed fewer ATF3 nuclei than the full crush group at both time points (**Figs. 6A and B**), consistent with the observations of reduced axotomy above. By day 30, ATF3 expression had reduced and become comparable between the groups (**Fig. 6B**). Levels of the microtubule-associated protein stathmin 2 (STMN2), a regulator of microtubule stability and neuronal growth after injury that colabels with ATF3 in the sensory ganglia^{26,78} was higher in the ipsilateral nerve after full crush injury, reaching statistical significance by day 7 (**Figs. 6C and D**). By day 30, the relative expression of STMN2 in the ipsilateral sciatic nerve reversed trend to higher levels in the partial crush model (Supplemental Figure 8A, available at <http://links.lww.com/PAIN/B843>). Growth-associated protein 43 (GAP-43) is expressed in the regenerating injured axons and nonmyelin forming Schwann cells.²² Correspondingly, we observed GAP-43 upregulation following crush injury, although levels were comparable between the full and partial crush models (Supplemental Figure 8B, C and D, available at <http://links.lww.com/PAIN/B843>).

We next investigated the injury profile of specific subpopulations of sensory neurons by performing double-labelling immunohistochemistry for ATF3 in ipsilateral L4 DRG with markers for the 3 major sensory neuron subtypes: Neurofilament 200 (NF200) a marker for large, myelinated, A β -fiber neurons; calcitonin-related gene peptide (CGRP), a marker for small-sized, c-fiber, peptidergic neurons, a subset of medium-sized A δ neurons; and isolectin B4 (IB4), a marker for small non-peptidergic c-fiber neurons⁶⁰ (**Fig. 6E**). Significantly fewer nuclei were ATF3 positive in each neuronal subset 2 days after partial crush compared with full crush injury: $49.2 \pm 1.9\%$ vs $62.3 \pm 3.1\%$ for NF200-positive neurons, $40.5 \pm 3.0\%$ vs $52.1 \pm 4.6\%$ CGRP-positive neurons, and $22.1 \pm 5.0\%$ vs $37.7 \pm 9.0\%$ for IB4-binding sensory neurons (**Fig. 6F**). When normalized to the total number of neurons in each subset, proportionally fewer IB4 neurons displayed ATF3 expression after partial crush compared with NF200 or CGRP subtypes (**Fig. 6G**). In summary, fewer axons of all types of sensory neurons expressed ATF3 after partial crush, likely reflecting the reduced axotomy compared with full crush.

3.8. Anatomy of axons after regeneration

To investigate the long-term changes to sciatic nerve anatomy, we analyzed myelinated axons in ultrathin sections of the distal nerve 30 days after crush injury in the 2 models (**Fig. 7A**). Myelinated axon profiles were distinguishable between all 3 groups (**Fig. 7B**). Myelinated axon density was significantly higher in the full crush model only (**Fig. 7C**), whereas the average g-ratio slope was significantly increased in both crush models compared with control (**Fig. 7D**). The average axon diameter was significantly lower (**Fig. 7E**) in the full crush nerve compared with partial crush and uninjured groups, with a corresponding shift to the left in axon diameters in the full crush group (**Fig. 7F**). By contrast, the average g-ratio was highest after partial crush (**Fig. 7G**), and g-ratios showed a right shift in distribution at day 30 compared with both the control and the full crush groups (**Fig. 7H**), suggesting thinner myelination in this group.

In addition to myelin thickness (g-ratio), changes to node length can also indicate potential changes to nerve conduction and pathophysiology.² However, no significant difference in nodal

length was observed between any groups (Supplemental Figure 9A and B, available at <http://links.lww.com/PAIN/B843>). These results suggest that abnormally thin myelination may be a lasting feature of a painful partial crush nerve injury.³⁶

4. Discussion

4.1. A novel neuropathic pain model

We report a robust focal nerve crush injury that reproducibly results in long-term hypersensitivity in mice of both sexes. We document the pathological changes to sensory afferent structure and function that we propose occur as a consequence of incomplete axonotmesis of the sciatic nerve. The survival and sparing of unmyelinated and smaller diameter myelinated fibers with partial crush nerve injury is consistent with a recently described incremental crush injury.⁴¹ Importantly, this paradigm helps fill a void in the preclinical literature regarding the link between clinically related traumatic nerve “crush” injury and neuropathic pain.

The advantage of the partial crush tool design is its simplicity and histologically defined effect on axon integrity. With as little as 30 μ m separating the blades of a crush tool, we show that the partial crush injury differs both phenotypically and anatomically from a fully crushed nerve. Together with the variability in blade apposition that we observed between commercially available tools, these divergent sensory phenotypes may help explain the discrepancies in prior literature regarding neuropathic pain-like behaviors in rodents after sciatic nerve crush.^{5,10,25,53}

The transient thermal and long-term tactile hypersensitivity after partial but not full crush injuries mirrors patients with painful and nonpainful traumatic partial nerve injury.⁵⁴ Our results suggest that these are in fact qualitatively different nerve injuries, helping explain why neuropathic outcomes do not necessarily correlate with either the severity of the injury^{18,63} or the magnitude of the systemic inflammatory response to tissue damage.⁶²

4.2. Persistent intact axons as a driver of neuropathic hypersensitivity

By comparing a “painful” partial crush with a full crush injury that did not evoke such behaviors,⁷⁹ we show that the persistent innervation of sensory axons following nerve injury is a defining feature before the development of hypersensitivity, homologous to historic observations of the chronic constriction injury model.³⁶

Denervation of the affected hind paw area was confirmed by a loss of retrograde Dil labelling in the corresponding DRG. One caveat with this approach is the diffuse nature of Dil labelling, which precluded the counting of individual DRG. Nevertheless, the lack of Dil signal in the L4 DRG after full crush injury confirms that Dil within the L4 DRG must have travelled through the sciatic nerve and not via another route.

Crush injury to the sciatic nerve is well known to result in the loss of nerve fibers in the skin that follows the time course of Wallerian degeneration.⁴³ Reduced IENF density is also a hallmark of small fiber neuropathy.⁵⁶ Although often painful, loss of IENF density does not necessarily correlate with painful symptoms.⁴⁷ In our study, the positive sensory function we observed after partial crush nerve injury correlated with the preservation of skin innervation, although IENF density was still lower than the uninjured paw. This suggests the presence of an inflection point where the sensory symptoms of progressive peripheral fiber loss transition from *hyperaesthesia* to *hypoesthesia*. Whether the spontaneous, paroxysmal-type pain

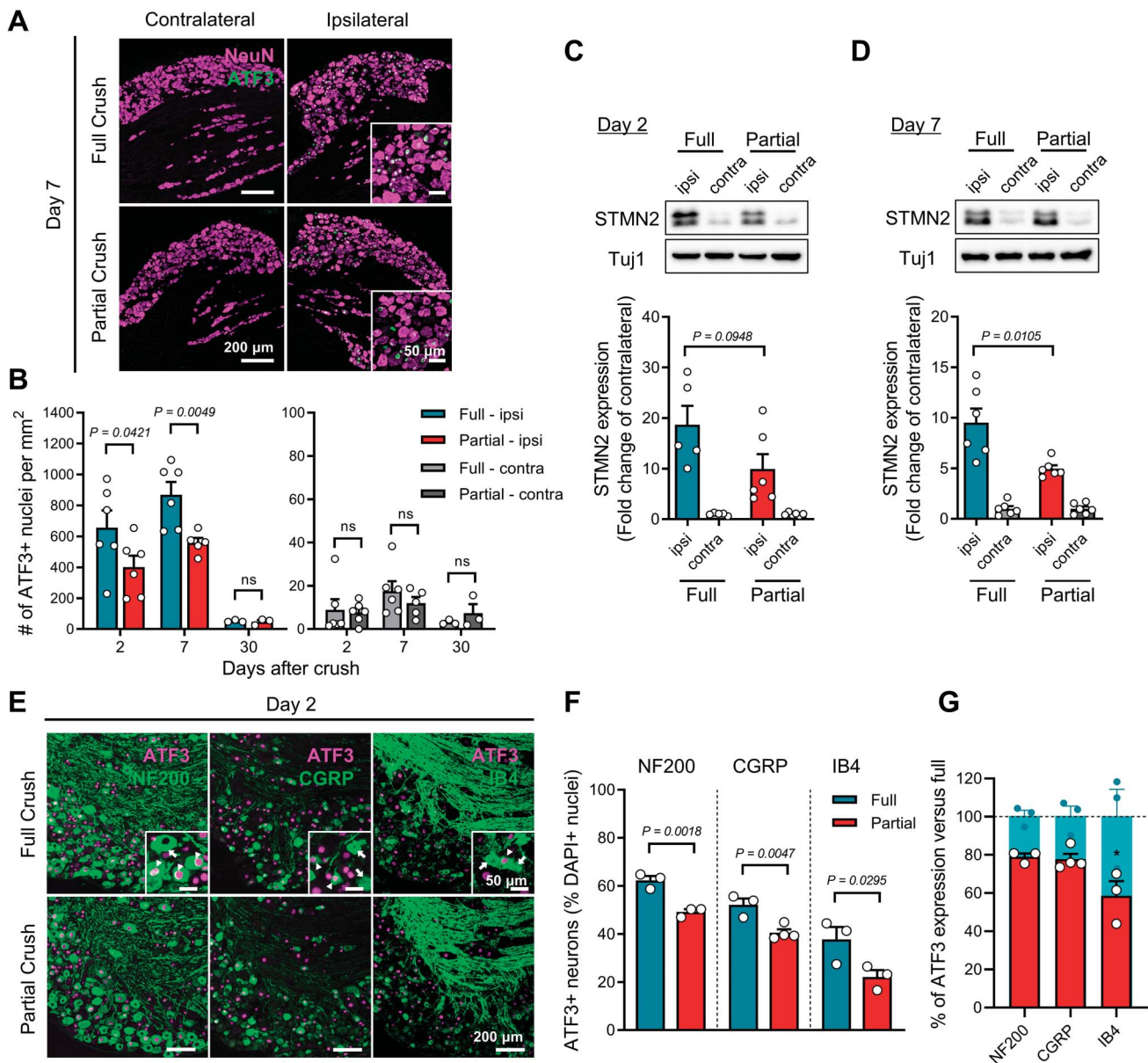


Figure 6. Axonal susceptibility to injury depends on sensory neuron subtype. (A) Representative ATF3 and NeuN staining image in L4 DRG on day 7. (B) Average number of ATF3-positive nuclei per NeuN-positive area on days 2, 7, and 30. $n = 3$ to 6 each group and time points. Unpaired t test. One-tailed. (C) Representative blot of STMN2 in sciatic nerve and the average of expression on day 2 and (D) day 7. Normalized with Tuj1 and fold change of the average contralateral expression is shown. $n = 5$ to 6 each group and time points. (E) Representative images of ATF3 and neuronal subpopulation markers (NF200, CGRP, IB4) on day 2. Arrowhead indicates neurons with ATF3-positive nuclei. Arrow indicates neurons without ATF3 expression. (F) Average percentage of ATF3 expression in each neuronal subtype. $n = 3$ to 4 each group and subtype. Unpaired t test. One-tailed. (G) Relative expression of ATF3 in the partial crush models normalized to the full crush group. Note that ATF3 expression in the IB4-binding neurons was significantly less than in the other 2 subtypes. One-way ANOVA with Tukey multiple comparison test. $F(2, 7) = 6.096$, $P = 0.0293$. * $P < 0.05$. P values are shown above each graph. Data are presented as mean \pm SEM. ATF3, activating transcription factor 3; CGRP, calcitonin-related gene peptide; DRG, dorsal root ganglia; IB4, isolectin B4; STMN2, stathmin 2.

associated with small fiber neuropathy is also a feature of the partial crush nerve injury remains to be investigated.

The milder sensory phenotype we observed after full crush nerve injury correlated with an almost complete denervation of the affected area, as confirmed by a loss of retrograde labelling to the corresponding DRG. Surgical resection of an injured nerve can be remarkably effective in achieving a meaningful reduction in pain in a proportion of patients.⁷⁰ Our phenotypic findings are corroborated by historical observations of Wallerian degeneration null (Wld) mice. Chronic constriction injury (CCI) in Wld mice, in which axons are preserved intact long after injury, resulted in less thermal sensitivity but prolonged mechanical hypersensitivity

compared with wild-type mice.⁸⁰ Thus, the removal of intact axons may in some cases reduce the likelihood of neuropathic pain after traumatic nerve injury.

The sparing of a proportion of axons from Wallerian degeneration after partial crush injury is also supported by the lower levels of NfL detected in the serum. NfL is now well established as a marker for neurodegeneration.⁴⁹ In mouse models, serum NfL levels are elevated as soon as 15 hours after sciatic nerve transection, with peak levels mainly attributed to Wallerian degeneration of axons.⁷⁴ Although the degenerative changes we observed in axon morphology on days 2 and 7 after partial crush appear delayed compared with the full crush, NfL levels

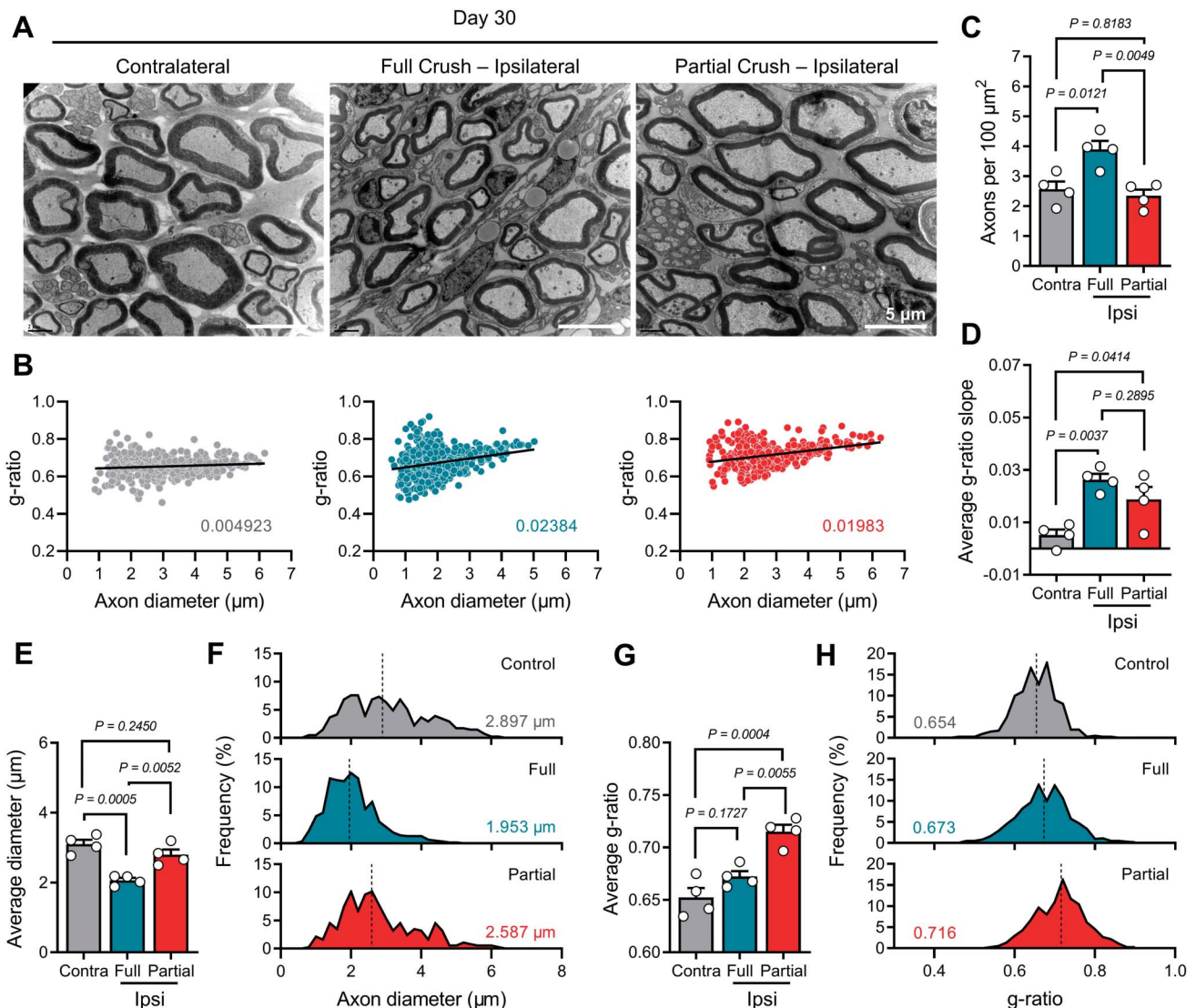


Figure 7. Exacerbated myelin-thinning in the partial crush nerve 30 days after injury. (A) Representative TEM images of the distal sciatic nerve on day 30 from male mice. (B) Scatterplot showing g-ratio as functions of axon diameter fitted with a linear function. The value inside each graph indicates the slope. (C) Number of myelinated axons per unit area. (D) Average slope of linear function. (E) Average diameter of the myelinated axons. (F) Frequency histogram of diameter. Contra vs Full: $D = 0.4217, P < 0.0001$, Contra vs Partial: $D = 0.1592, P < 0.0001$, Full vs Partial: $D = 0.3522, P < 0.0001$. (G) Average g-ratio of the axons. (H) Frequency histogram of g-ratio. Contra vs Full: $D = 0.1992, P < 0.0001$, Contra vs Partial: $D = 0.4432, P < 0.0001$, Full vs Partial: $D = 0.2738, P < 0.0001$. (C–E, G) One-way ANOVA with Tukey multiple comparison test. P values are shown above each graph. $n = 4$ mice per group. Data are presented as means \pm SEM. (F and H). The dashed line and the value inside each graph indicate the median of each group. Two sample Kolmogorov–Smirnov test. Two-sided. Contra $n = 410$, Full $n = 623$, Partial $n = 375$ axons.

returned to baseline within a week after both injuries, suggesting that the surviving axons escape Wallerian degeneration altogether rather than delay until later time points.

The Wallerian degeneration and inflammatory environment of the injured nerve is expected to drive phenotypic changes in the axons remaining intact after partial crush injury.⁵⁸ Although the sensory neuron subtype(s) driving the chronic tactile hypersensitivity remains unclear, this work does provide several clues to their identity. The greatest proportion of ATF3-expressing DRG neurons after both crush injuries were NF200+ large-size neurons. This result is consistent with reports that large axons are more susceptible to traumatic injury.^{36,40,57,81} Indeed, in both crush models, there was an almost complete loss of myelinated axons larger than 4 μm , which would include all A α (12–10 μm) and A β (6–12 μm) fibres but spare a proportion of A δ afferents (1–6 μm).^{35,87} However, just more than half of the IB4-binding

neurons expressed ATF3 early after partial crush injury, suggesting that these small-sized and unmyelinated nonpeptidergic neurons may be more likely to escape the initial injury. IB4+ neurons are associated with expression of the mas-related G-protein-coupled receptor member D (Mrgprd) and have been implicated in conveying sensitivity to noxious mechanical stimuli and mechanical allodynia¹⁴ after peripheral nerve injury,⁸⁶ as well aberrant sprouting into low-threshold mechanically sensitive peripheral end organs in the dermis.³⁴

4.3. A mixed inflammatory and neuropathic pain model?

Partial crush injury was also typified by a transient and resolving hypersensitivity to heat. The evidence for thermal hypersensitivity following traumatic nerve injury varies between the models. For example, the latency to withdrawal from heat in rats is reduced

after chronic constriction injury (CCI)¹⁰ but not after spared nerve injury (SNI)²⁶; the former is thought to involve a stronger inflammatory component.⁴⁴ Traumatic nerve injury elicits a strong inflammatory response within the nerve,³¹ and it is likely that intact, small-diameter nociceptors passing through this inflammatory milieu after partial crush become sensitized leading to the observed lowering in thermal thresholds.⁵⁸ IB4+ neurons, which appeared to remain the most intact following partial crush injury, are also thought to increase capsaicin (TRPV1 agonist) responsiveness under inflammatory conditions.¹³ The resolution of thermal but not mechanical hypersensitivity we observed after 28 days in the partial crush model therefore appears to suggest the transition from an inflammatory to a neuropathic state around this time point that parallels other chronic pain models.¹⁷

4.4. Crush-induced neuropathic pain: a maladaptive response of regeneration?

The increase in myelinated axon density and reduction in axon diameter we observed more than 30 days after full crush injury is a well-reported characteristic of axons after injury and regeneration.⁷³ Axons are known to possess thinner myelin after regeneration,¹² and prolonged myelin thinning may indicate impaired regeneration.⁴⁶ Interestingly, partial crush resulted in a significantly greater g-ratio compared with full crush. Schwann cells form myelin sheaths to provide support to the axon,²⁹ and Schwann cell demyelination may induce a transcriptional injury response in sensory neurons.³⁰ Whether the ongoing myelin disturbance reflects a pathological response of Schwann cells to the injury or is a consequence of a persistent underlying axon pathology is currently unknown. Interestingly, the thinner myelination after partial crush injury coincides with higher levels of the injury marker STMN2, suggesting that some axons may exist in a persistent injury or regenerative state.⁸⁸

4.5. Therapeutic targeting of partial crush injury-induced neuropathic pain

Aberrant myelination has been implicated in various neuropathic conditions, and several studies show that demyelination is both sufficient and necessary to transform touch into pain.^{27,38} Therefore, promoting myelin repair may reduce sensory hypersensitivity after peripheral nerve injury.^{32,89}

Recent clinical evidence suggests that improved regeneration correlates with a functional recovery after release of a compressed nerve,⁸ thus targeting neurotrophic factors to enhance axon regeneration may have therapeutic benefit. Conversely, precision ablation of intact, pathogenic, small-sized sensory afferents, either by genetic³⁴ or immunological²³ methods may offer an alternative targeted approach to the resolution of a neuropathic sensory phenotype.

We conclude that incomplete axonotmesis (ie, partial crush) and the persistence of intact afferents through a nerve injury site are significant risk factors for persistent neuropathic pain⁴⁸ and reinforces the differential mechanisms underlying the development of different pain types.³³ It is important to note that translation of these findings from mice to humans must account for the considerable distance and time over which axon regeneration occurs in human nerve injury.⁷⁵ Nevertheless, we believe that this study offers a useful method to explore the pathomechanisms of a clinically relevant nerve injury and dissect the unique characteristics of a painful nerve.

Conflict of interest statement

The authors have no conflict of interest to declare.

Acknowledgements

The authors thank Chan Hee Won, our previous laboratory assistant, for critical assistance in behavior experiments, Dr. Dae-Hyun Roh at the Kyung Hee University for assistance with rotor-rod testing, and Dr. Yong Ho Kim at the Gachon University and Dr. Pa Reum Lee at the Korea Institute of Science and Technology for assistance with nerve tracing. The authors thank Hyoung Yon Kim at the Korea University for statistical support on single-axon analysis and Dr. Shuaiwei Wang for assistance with behavioral experiments. The authors thank Kyle Hallett and Joseph Tacon at the Oxford Departments of Oncology and Physics, respectively, for their assistance with the haemostat customisation and quality control measurements. The authors also thank Charlotte Melia and the team at the Sir William Dunn School of Pathology Bioimaging Facility for their assistance with TEM. The authors are especially grateful to Dr. Hwan Tae Park, Dr. Jung Eun Shin, Dr. Ahmet Hoke, Dr. Annina Schmid, Dr. Alban Latremoliere, and Dr. Michael Costigan for helpful advice and discussion on peripheral nerve anatomy and analysis and the partial crush injury model. This research was supported by the National Research Foundation of Korea grants (NRF-2018R1A5A2024418 and NRF-2021R1A2C3003334) funded by the Korean government MSIT (Ministry of Science and ICT) to S. B. Oh, a UKRI Future Leaders Fellowship grant (MR/V02552X/1) to A. J. Davies, Medical Research Council UK (MR/P008399/1) to S. Rinaldi, and Medical Research Council UK (MR/T020113/1) to D. L. H. Bennett. A. J. Davies also receives support from the Children's Cancer and Leukaemia Group (CCLG) (CCLGA 2022 05). For the purpose of Open Access, the authors have applied a CC BY public copyright licence to any Author Accepted Manuscript (AAM) version arising from this submission.

Author contributions: Conceptualization: H. W. Kim, A. J. Davies, and S. B. Oh; Methodology: H. W. Kim, A. J. Davies, E. Johnson, S. J. Middleton, Y. C. Bae, M. J. A. Koel-Simmelink, L. Wieske, C. E. Teunissen, M. Tacon, and J. Prentice; Investigation: H. W. Kim, A. J. Davies, S. W. Shim, H. M. Han, W. Kim, S. Chung, A. M. Zhao, D. Roh, E. Johnson, M. J. A. Koel-Simmelink, and L. Wieske; Resources: C. E. Teunissen, Y. C. Bae, D. L.H. Bennett, S. Rinaldi, A. J. Davies, and S. B. Oh; Writing (original draft): H. W. Kim and A. J. Davies; Writing (editing): H. W. Kim, S. J. Middleton, C. E. Teunissen, D. L. H. Bennett, S. Rinaldi, A. J. Davies, and S. B. Oh; Project supervision: A. J. Davies and S. B. Oh.

Supplemental digital content

Supplemental digital content associated with this article can be found online at <http://links.lww.com/PAIN/B843>.

Article history:

Received 17 October 2022

Received in revised form 5 April 2023

Accepted 12 April 2023

Available online 27 June 2023

References

- [1] Alvites RD, Rita Caseiro A, Santos Pedrosa S, Vieira Branquinho M, Ronchi G, Geuna S, Varejão ASP, Colette Mauricio A. Peripheral nerve

- injury and axonotmesis: state of the art and recent advances. *Cogent Med* 2018;5:1466404.
- [2] Arancibia-Carcamo IL, Ford MC, Cossell L, Ishida K, Tohyama K, Attwell D. Node of Ranvier length as a potential regulator of myelinated axon conduction speed. *Elife* 2017;6:e23329.
 - [3] Arnold TB, Emerson JW. Nonparametric Goodness-of-Fit tests for discrete null distributions. *R J* 2011;3:34–9.
 - [4] Attal N, Bouhassira D. Translational neuropathic pain research. *PAIN* 2019;160:S23–8.
 - [5] Attal N, Filliatreau G, Perrot S, Jazat F, Di Giambardino L, Guilbaud G. Behavioural pain-related disorders and contribution of the saphenous nerve in crush and chronic constriction injury of the rat sciatic nerve. *PAIN* 1994;59:301–12.
 - [6] Austin PJ, Moalem-Taylor G. Animal models of neuropathic pain due to nerve injury. *Neuromethods* 2013;78:239–60.
 - [7] Bain JR, Mackinnon SE, Hunter DA. Functional evaluation of complete sciatic, peroneal, and posterior tibial nerve lesions in the rat. *Plast Reconstr Surg* 1989;83:137–8.
 - [8] Baskozos G, Sandy-Hindmarch O, Clark AJ, Windsor K, Karlsson P, Weir GA, McDermott LA, Burchall J, Wiberg A, Furniss D, Bennett DLH, Schmid AB. Molecular and cellular correlates of human nerve regeneration: ADCYAP1/PACAP enhance nerve outgrowth. *Brain* 2020;143:2009–26.
 - [9] Bate ST, Clark RA. The design and statistical analysis of animal experiments. Cambridge, United Kingdom: Cambridge University Press, 2014.
 - [10] Bennett GJ, Xie YK. A peripheral mononeuropathy in rat that produces disorders of pain sensation like those seen in man. *PAIN* 1988;33:87–107.
 - [11] Bester H, Beggs S, Woolf CJ. Changes in tactile stimuli-induced behavior and c-Fos expression in the superficial dorsal horn and in parabrachial nuclei after sciatic nerve crush. *J Comp Neurol* 2000;428:45–61.
 - [12] Beuche W, Friede RL. A new approach toward analyzing peripheral nerve fiber populations. II. Foreshortening of regenerated internodes corresponds to reduced sheath thickness. *J Neuropathol Exp Neurol* 1985;44:73–84.
 - [13] Breese NM, George AC, Pauers LE, Stucky CL. Peripheral inflammation selectively increases TRPV1 function in IB4-positive sensory neurons from adult mouse. *PAIN* 2005;115:37–49.
 - [14] Cavanaugh DJ, Lee H, Lo L, Shields SD, Zylka MJ, Basbaum AI, Anderson DJ. Distinct subsets of unmyelinated primary sensory fibers mediate behavioral responses to noxious thermal and mechanical stimuli. *Proc Natl Acad Sci U S A* 2009;106:9075–80.
 - [15] Chen LE, Seaber AV, Glisson RR, Davies H, Murrell GA, Anthony DC, Urbaniak JR. The functional recovery of peripheral nerves following defined acute crush injuries. *J Orthop Res* 1992;10:657–64.
 - [16] Chen LE, Seaber AV, Urbaniak JR. The influence of magnitude and duration of crush load on functional recovery of the peripheral nerve. *J Reconstr Microsurg* 1993;9:299–306; discussion 306–7.
 - [17] Christianson CA, Corr M, Firestein GS, Mobargha A, Yaksh TL, Svensson CI. Characterization of the acute and persistent pain state present in K/BxN serum transfer arthritis. *PAIN* 2010;151:394–403.
 - [18] Ciaramitaro P, Padua L, Devigili G, Rota E, Tamburin S, Eleopra R, Cruccu G, Truini A; Neuropathic Pain Special Interest Group of the Italian Neurological Society. Prevalence of neuropathic pain in patients with traumatic brachial plexus injury: a multicenter prospective hospital-based study. *Pain Med* 2017;18:2428–32.
 - [19] Cohen SP, Vase L, Hooten WM. Chronic pain: an update on burden, best practices, and new advances. *Lancet* 2021;397:2082–97.
 - [20] Coleman MP, Freeman MR. Wallerian degeneration, wld(s), and nmnat. *Annu Rev Neurosci* 2010;33:245–67.
 - [21] Crombie IK, Davies HT, Macrae WA. Cut and thrust: antecedent surgery and trauma among patients attending a chronic pain clinic. *PAIN* 1998;76:167–71.
 - [22] Curtis R, Stewart HJ, Hall SM, Wilkin GP, Mirsky R, Jessen KR. GAP-43 is expressed by nonmyelin-forming Schwann cells of the peripheral nervous system. *J Cell Biol* 1992;116:1455–64.
 - [23] Davies AJ, Kim HW, Gonzalez-Cano R, Choi J, Back SK, Roh SE, Johnson E, Gabriac M, Kim MS, Lee J, Lee JE, Kim YS, Bae YC, Kim SJ, Lee KM, Na HS, Riva P, Latremoliere A, Rinaldi S, Ugolini S, Costigan M, Oh SB. Natural killer cells degenerate intact sensory afferents following nerve injury. *Cell* 2019;176:716–28.e18.
 - [24] de Lange JWD, Duraku LS, Power DM, Rajaratnam V, van der Oest MJW, Selles RW, Huygen F, Hundepool CA, Zuidam JM. Prevalence of post-traumatic neuropathic pain after digital nerve repair and finger amputation. *J Plast Reconstr Aesthet Surg* 2022;75:3242–9.
 - [25] Decosterd I, Allchorne A, Woolf CJ. Progressive tactile hypersensitivity after a peripheral nerve crush: non-noxious mechanical stimulus-induced neuropathic pain. *PAIN* 2002;100:155–62.
 - [26] Decosterd I, Woolf CJ. Spared nerve injury: an animal model of persistent peripheral neuropathic pain. *PAIN* 2000;87:149–58.
 - [27] Ding YQ, Qi JG. Sensory root demyelination: transforming touch into pain. *Glia* 2022;70:397–413.
 - [28] Dubovy P, Klusakova I, Hradilova-Svizenska I, Joukal M. Expression of regeneration-associated proteins in primary sensory neurons and regenerating axons after nerve injury—an overview. *Anat Rec (Hoboken)* 2018;301:1618–27.
 - [29] Duncan ID, Marik RL, Broman AT, Heidari M. Thin myelin sheaths as the hallmark of remyelination persist over time and preserve axon function. *Proc Natl Acad Sci U S A* 2017;114:E9685–91.
 - [30] Elbaz B, Yang L, Vardy M, Isaac S, Rader BL, Kawaguchi R, Traka M, Woolf CJ, Renthal W, Popko B. Sensory neurons display cell-type-specific vulnerability to loss of neuron-glia interactions. *Cell Rep* 2022;40:111130.
 - [31] Ellis A, Bennett DL. Neuroinflammation and the generation of neuropathic pain. *Br J Anaesth* 2013;111:26–37.
 - [32] Endo T, Kadoya K, Suzuki T, Suzuki Y, Terkawi MA, Kawamura D, Iwasaki N. Mature but not developing Schwann cells promote axon regeneration after peripheral nerve injury. *NPJ Regen Med* 2022;7:12.
 - [33] Finnerup NB, Nikolajsen L, Rice ASC. Transition from acute to chronic pain: a misleading concept? *PAIN* 2022;163:e985–8.
 - [34] Gangadharan V, Zheng H, Taberner FJ, Landry J, Nees TA, Pistolic J, Agarwal N, Mannich D, Benes V, Helmstaedter M, Ommer B, Lechner SG, Kuner T, Kuner R. Neuropathic pain caused by miswiring and abnormal end organ targeting. *Nature* 2022;606:137–45.
 - [35] Gasser HS, Grundfest H. Axon diameters in relation to the spike dimensions and the conduction velocity in mammalian A fibers. *Am J Physiol Legacy Content* 1939;127:393–414.
 - [36] Gautron M, Jazat F, Ratinahirana H, Hauw JJ, Guilbaud G. Alterations in myelinated fibres in the sciatic nerve of rats after constriction: possible relationships between the presence of abnormal small myelinated fibres and pain-related behaviour. *Neurosci Lett* 1990;111:28–33.
 - [37] Geary MB, Li H, Zingman A, Ketz J, Zuscik M, De Mesy Bentley KL, Noble M, Elfar JC. Erythropoietin accelerates functional recovery after moderate sciatic nerve crush injury. *Muscle Nerve* 2017;56:143–51.
 - [38] Gillespie CS, Sherman DL, Fleetwood-Walker SM, Cottrell DF, Tait S, Garry EM, Wallace VC, Ure J, Griffiths IR, Smith A, Brophy PJ. Peripheral demyelination and neuropathic pain behavior in periaxin-deficient mice. *Neuron* 2000;26:523–31.
 - [39] Goebbels S, Oltrogge JH, Kemper R, Heilmann I, Bormuth I, Wolfer S, Wichert SP, Mobius W, Liu X, Lappe-Siefke C, Rossner MJ, Groszer M, Suter U, Frahm J, Boretius S, Nave KA. Elevated phosphatidylinositol 3,4,5-trisphosphate in glia triggers cell-autonomous membrane wrapping and myelination. *J Neurosci* 2010;30:8953–64.
 - [40] Haftek J, Thomas PK. Electron-microscope observations on the effects of localized crush injuries on the connective tissues of peripheral nerve. *J Anat* 1968;103:233–43.
 - [41] Hamad MN, Boroda N, Echenique DB, Dieter RA, Amirouche FML, Gonzalez LH, Kems JM. Compound motor action potentials during a modest nerve crush. *Front Cell Neurosci* 2022;16:798203.
 - [42] Haroutunian S, Nikolajsen L, Finnerup NB, Jensen TS. The neuropathic component in persistent postsurgical pain: a systematic literature review. *PAIN* 2013;154:95–102.
 - [43] Hsieh ST, Chiang HY, Lin WM. Pathology of nerve terminal degeneration in the skin. *J Neuropathol Exp Neurol* 2000;59:297–307.
 - [44] Hu P, Bembrick AL, Keay KA, McLachlan EM. Immune cell involvement in dorsal root ganglia and spinal cord after chronic constriction or transection of the rat sciatic nerve. *Brain Behav Immun* 2007;21:599–616.
 - [45] Huang C, Zou W, Lee K, Wang E, Zhu X, Guo Q. Different symptoms of neuropathic pain can be induced by different degrees of compressive force on the C7 dorsal root of rats. *Spine J* 2012;12:1154–60.
 - [46] Jha MK, Passero JV, Rawat A, Ament XH, Yang F, Vidensky S, Collins SL, Horton MR, Hoke A, Rutter GA, Latremoliere A, Rothstein JD, Morrison BM. Macrophage monocarboxylate transporter 1 promotes peripheral nerve regeneration after injury in mice. *J Clin Invest* 2021;131:e141964.
 - [47] Karlsson P, Hincker AM, Jensen TS, Freeman R, Haroutunian S. Structural, functional, and symptom relations in painful distal symmetric polyneuropathies: a systematic review. *PAIN* 2019;160:286–97.
 - [48] Kehlet H, Jensen TS, Woolf CJ. Persistent postsurgical pain: risk factors and prevention. *Lancet* 2006;367:1618–25.
 - [49] Khalil M, Teunissen CE, Otto M, Pielh F, Sormani MP, Gatteringer T, Barro C, Kappos L, Comabella M, Fazekas F, Petzold A, Blennow K, Zetterberg H, Kuhle J. Neurofilaments as biomarkers in neurological disorders. *Nat Rev Neurol* 2018;14:577–89.
 - [50] Kim HW, Won CH, Oh SB. Lack of correlation between spinal microgliosis and long-term development of tactile hypersensitivity in

- two different sciatic nerve crush injury. *Mol Pain* 2021;17:174480692110113.
- [51] Kim SH, Chung JM. An experimental model for peripheral neuropathy produced by segmental spinal nerve ligation in the rat. *PAIN* 1992;50:355–63.
- [52] Ko MH, Yang ML, Youn SC, Lan CT, Tseng TJ. Intact subepidermal nerve fibers mediate mechanical hypersensitivity via the activation of protein kinase C gamma in spared nerve injury. *Mol Pain* 2016;12:174480691665618.
- [53] Lancelotta MP, Sheth RN, Meyer RA, Belzberg AJ, Griffin JW, Campbell JN. Severity and duration of hyperalgesia in rat varies with type of nerve lesion. *Neurosurgery* 2003;53:1200–9; discussion 1208–9.
- [54] Landerholm ÅH, Ekblom AG, Hansson PT. Somatosensory function in patients with and without pain after traumatic peripheral nerve injury. *Eur J Pain* 2010;14:847–53.
- [55] Lauria G, Cornblath DR, Johansson O, McArthur JC, Mellgren SI, Nolano M, Rosenberg N, Sommer C; European Federation of Neurological Societies. EFNS guidelines on the use of skin biopsy in the diagnosis of peripheral neuropathy. *Eur J Neurol* 2005;12:747–58.
- [56] Lauria G, Faber CG, Cornblath DR. Skin biopsy and small fibre neuropathies: facts and thoughts 30 years later. *J Neurol Neurosurg Psychiatry* 2022;93:915–8.
- [57] Lee JC. Electron microscopy of Wallerian degeneration. *J Comp Neurol* 1963;120:65–79.
- [58] Lemaître D, Hurtado ML, De Gregorio C, Onate M, Martinez G, Catenaccio A, Wishart TM, Court FA. Collateral sprouting of peripheral sensory neurons exhibits a unique transcriptomic profile. *Mol Neurobiol* 2020;57:4232–49.
- [59] Mangus LM, Rao DB, Ebenezer GJ. Intraepidermal nerve fiber analysis in human patients and animal models of peripheral neuropathy: a comparative review. *Toxicol Pathol* 2020;48:59–70.
- [60] McCoy ES, Taylor-Blake B, Street SE, Pribisko AL, Zheng J, Zylka MJ. Peptidergic CGRP α primary sensory neurons encode heat and itch and tonically suppress sensitivity to cold. *Neuron* 2013;78:138–51.
- [61] Menorca RM, Fussell TS, Elfar JC. Nerve physiology: mechanisms of injury and recovery. *Hand Clin* 2013;29:317–30.
- [62] Miculescu AA, Granlund P, Butler S, Gordh T. Association between systemic inflammation and experimental pain sensitivity in subjects with pain and painless neuropathy after traumatic nerve injuries. *Scand J Pain* 2022;23:184–99.
- [63] Mikkelsen T, Werner MU, Lassen B, Kehlet H. Pain and sensory dysfunction 6 to 12 months after inguinal herniotomy. *Anesth Analg* 2004;99:146–51.
- [64] Miranda GE, Torres RY. Epidemiology of traumatic peripheral nerve injuries evaluated with electrodiagnostic studies in a tertiary care hospital clinic. *P R Health Sci J* 2016;35:76–80.
- [65] National Research Council (US) Committee for the Update of the Guide for the Care and Use of Laboratory Animals. Guide for the care and use of laboratory animals. 8th ed. Washington, DC: National Academies Press (US), 2011.
- [66] Omura T, Sano M, Omura K, Hasegawa T, Nagano A. A mild acute compression induces neuropathic pain in rat sciatic nerve. *Int J Neurosci* 2004;114:1561–72.
- [67] Padovano WM, Dengler J, Patterson MM, Yee A, Snyder-Warwick AK, Wood MD, Moore AM, Mackinnon SE. Incidence of nerve injury after extremity trauma in the United States. *Hand (N Y)* 2022;17:615–23.
- [68] Percie du Sert N, Hurst V, Ahluwalia A, Alam S, Avey MT, Baker M, Browne WJ, Clark A, Cuthill IC, Dirnagl U, Emerson M, Garner P, Holgate ST, Howells DW, Karp NA, Lazic SE, Lidster K, MacCallum CJ, Macleod M, Pearl EJ, Petersen OH, Rawle F, Reynolds P, Rooney K, Sena ES, Silberberg SD, Steckler T, Wurbel H. The ARRIVE guidelines 2.0: updated guidelines for reporting animal research. *Br J Pharmacol* 2020;177:3617–24.
- [69] Percie du Sert N, Rice AS. Improving the translation of analgesic drugs to the clinic: animal models of neuropathic pain. *Br J Pharmacol* 2014;171:2951–63.
- [70] Poppler LH, Parikh RP, Bichanich MJ, Rebehn K, Bettlach CR, Mackinnon SE, Moore AM. Surgical interventions for the treatment of painful neuroma: a comparative meta-analysis. *PAIN* 2018;159:214–23.
- [71] Razaq S, Yasmeen R, Butt AW, Akhtar N, Mansoor SN. The pattern of peripheral nerve injuries among Pakistani soldiers in the war against terror. *J Coll Phys Surg Pak* 2015;25:363–6.
- [72] Sandelius A, Zetterberg H, Blennow K, Adiatori R, Malaspina A, Laura M, Reilly MM, Rossor AM. Plasma neurofilament light chain concentration in the inherited peripheral neuropathies. *Neurology* 2018;90:e518–24.
- [73] Sanders FK, Hardy AC. The thickness of the myelin sheaths of normal and regenerating peripheral nerve fibres. *Proc R Soc Lond Ser B Biol Sci* 1948;135:323–57.
- [74] Sasaki Y, Engber TM, Hughes RO, Figley MD, Wu T, Bosanac T, Devraj R, Milbrandt J, Krauss R, DiAntonio A. cADPR is a gene dosage-sensitive biomarker of SARM1 activity in healthy, compromised, and degenerating axons. *Exp Neurol* 2020;329:113252.
- [75] Scheib J, Hoke A. Advances in peripheral nerve regeneration. *Nat Rev Neurol* 2013;9:668–76.
- [76] Seddon HJ. Three types of nerve injury. *Brain* 1943;66:237–88.
- [77] Seltzer Z, Dubner R, Shir Y. A novel behavioral model of neuropathic pain disorders produced in rats by partial sciatic nerve injury. *PAIN* 1990;43:205–18.
- [78] Shin JE, Geisler S, DiAntonio A. Dynamic regulation of SCG10 in regenerating axons after injury. *Exp Neurol* 2014;252:1–11.
- [79] Sommer C, Myers RR. Neurotransmitters in the spinal cord dorsal horn in a model of painful neuropathy and in nerve crush. *Acta Neuropathol* 1995;90:478–85.
- [80] Sommer C, Schäfers M. Painful mononeuropathy in C57BL/6J mice with delayed wallerian degeneration: differential effects of cytokine production and nerve regeneration on thermal and mechanical hypersensitivity. *Brain Res* 1998;784:154–62.
- [81] Strain RE, Olson WH. Selective damage of large diameter peripheral nerve fibers by compression: an application of Laplace's law. *Exp Neurol* 1975;47:68–80.
- [82] Sunderland S. A classification of peripheral nerve injuries producing loss of function. *Brain* 1951;74:491–516.
- [83] Taylor CA, Braza D, Rice JB, Dillingham T. The incidence of peripheral nerve injury in extremity trauma. *Am J Phys Med Rehabil* 2008;87:381–5.
- [84] Tsujino H, Kondo E, Fukuoka T, Dai Y, Tokunaga A, Miki K, Yonenobu K, Ochi T, Noguchi K. Activating transcription factor 3 (ATF3) induction by axotomy in sensory and motoneurons: a novel neuronal marker of nerve injury. *Mol Cell Neurosci* 2000;15:170–82.
- [85] Vogelaar CF, Vrinten DH, Hoekman MF, Brakkee JH, Burbach JP, Hamers FP. Sciatic nerve regeneration in mice and rats: recovery of sensory innervation is followed by a slowly retreating neuropathic pain-like syndrome. *Brain Res* 2004;1027:67–72.
- [86] Warwick C, Cassidy C, Hachisuka J, Wright MC, Baumbauer KM, Adelman PC, Lee KH, Smith KM, Sheahan TD, Ross SE, Koerber HR. MrgprdCre lineage neurons mediate optogenetic allodynia through an emergent polysynaptic circuit. *PAIN* 2021;162:2120–31.
- [87] Whitwam JG. Classification of peripheral nerve fibres. An historical perspective. *Anaesthesia* 1976;31:494–503.
- [88] Xie W, Strong JA, Zhang JM. Active nerve regeneration with failed target reinnervation drives persistent neuropathic pain. *eNeuro* 2017;4:ENEURO.0008-17.2017.
- [89] Zhou Y, Notterpek L. Promoting peripheral myelin repair. *Exp Neurol* 2016;283:573–80.